ASSESSMENT OF PARTIAL STRAND DEBONDING PRACTICE FOR AASHTO TYPE GIRDERS

by

Weijin Wang

Bachelor of Engineering, Southwest JiaoTong University, 2011

Submitted to the Graduate Faculty of

Swanson School of Engineering in partial fulfillment

of the requirements for the degree of

Master of Science

University of Pittsburgh

2013

UNIVERSITY OF PITTSBURGH

SWANSON SCHOOL OF ENGINEERING

This thesis was presented

by

Weijin Wang

It was defended on

July 2, 2013

and approved by

Dr. John Brigham, Ph.D., Assistant Professor, Department of Civil and Environmental Engineering

Dr. Qiang Yu, Ph.D., Assistant Professor, Department of Civil and Environmental Engineering

Thesis Advisor: Dr. Kent A. Harries, Ph.D., Associate Professor, Department of Civil and Environmental Engineering

ASSESSMENT OF PARTIAL STRAND DEBONDING PRACTICE FOR AASHTO TYPE GIRDERS

Weijin Wang, M.S.

University of Pittsburgh, 2013

Pretensioned girders have been commonly used in bridge construction for years. However, some problems remain that hinder the further application of longer and more heavily prestressed girders. The prestressing force can produce large stresses at both the top and bottom surfaces of the girders, especially near the ends where self-weight moments are minimal. Additionally, the transfer of large prestressing forces can cause local cracking. Partial debonding of straight strands, harping strands and/or adding top strands are three common approaches to mitigating such problems. However, harping is limited to those strands aligned with the member web, and adding top strands affects the overall stress state of the section. Comparatively, partial debonding is a simple and preferred approach. The total prestress force is introduced to the member gradually, reducing stress concentrations and associated end-region cracking.

Even so, partial debonding decreases the longitudinal tension capacity particularly when a large number of strands is debonded. Excessive debonding, therefore, can also have detrimental effects of the flexure and shear capacity of the girder. This thesis aims to quantify the effects of partial debonding on initial girder stresses and ultimate girder capacity in an effort to identify acceptable prestressing strand debonding details.

Two series of AASHTO Type III-VI girders having varying spans, amounts of prestressing and different debonding ratios are systematically analysed for their adherence and

consistency with present AASHTO *LRFD Specification* requirements. The analyses use a purpose-written MATLAB program. Analytically obtained girder capacities are validated with initial design capacities from the *PCI Bridge Design Manual*. An individual case is presented in order to illustrate the analysis procedure. From this study, acceptable partial debonding ranges, satisfying AASHTO-prescribed stress limits, are obtained.

Conclusions indicate that the upper limit for an acceptable debonding ratio may be increased from the AASHTO-prescribed 25% to perhaps 50%. However the results also indicate that this upper limit is a function of span length and may be greater for longer spans. In many cases no acceptable amount of debonding was found for shorter spans. Further parametric study is required to establish such a relationship and to extend the study to other girder shapes.

TABLE OF CONTENTS

LIST OF TABLES

LIST OF FIGURES

NOMENCLATURE

The following abbreviations and notation are used in this work.

Abbreviations

AASHTO	American Association of State Highway and Transportation Officials
FEM	Finite Element Method
LRFD	Load and Resistance Factor Design
MCFT	Modified Compression Field Theory
PCI	Precast/Prestressed Concrete Institute

Notation

A	girder section area
A_{cg}	concrete cross sectional area
A_{ps}	prestressed reinforcement area in the tension zone
A_s	area of nonprestressed tension reinforcement
A_v	area of a transverse reinforcement within distance s
b	width of compression face of member
b_v	section web breadth
b_w	width member web(s)
DC	AASHTO-prescribed dead load of permanent components

DW	AASHTO-prescribed wearing surface load
d_b	nominal diameter of prestressing strand
d_v	section web depth; effective shear depth
d_r	maximum debonding ratio
E_c	modulus of elasticity of concrete
E_p	tensile modulus of elasticity of prestressing steel, taken as 28500 ksi
e	eccentricity of prestressing steel with respect to centroidal axis of member
f_c	concrete stress
f_c'	specified compressive strength of concrete
f_{ci}	concrete compressive stress at prestress transfer
f_{pb}	compressive stress due to effective prestress
f_{pe}	effective prestress in prestressed steel reinforcement
f_{pi}	initial prestressing force
f_{ps}	stress in prestressed reinforcement at nominal strength
f_{pu}	specified tensile strength of prestressing tendons
f_y	specified minimum yield strength of reinforcing bars
H	girder depth
I	moment of Inertia
IM	AASHTO-prescribed vehicular impact load
L	span length
LL	AASHTO-prescribed vehicular live load
l_d	development length
l_t	transfer length

M	moment due to eccentric prestressing force in strands
M_{cr}	cracking moment
M_{DC}	moment on girder due to dead load components and attachments
M_D	moment on girder due to dead load components (including member self-weight) and attachments
M_{DW}	moment on girder due to wearing surface
M_n	nominal flexural strength of girder
M_u	design ultimate flexural strength of girder
N	total number of strands
N_u	applied factored axial force taken as positive if tensile
P	prestress force
S	section elastic modulus (Eq. 2-3); center-to-center girder spacing
S_b	section modulus of the bottom of the member
S_t	section modulus of the top of the member
s	spacing of reinforcing bars
T	total tension force
T_v	additional tensile force in the longitudinal reinforcement
t_s	thickness of slab
V_c	nominal shear resistance provided by tensile stresses in the concrete
V_n	nominal shear resistance of the section considered
V_p	component in the direction of the applied shear of the effective prestressing force; positive if resisting the applied shear
V_s	shear resistance provided by shear reinforcement

V_u	factored shear force at section
w	Girder Self Weight
y_b	distance from extreme bottom fiber to the section centroid
y_t	empirical constant to determine an equivalent rectangular stress distribution in concrete
β	factor relating effect of longitudinal strain on the shear capacity of concrete, as indicated by the ability of diagonally cracked concrete to transmit tension
Δf_{pES}	prestress loss due to elastic shortening
Δf_{pLT}	prestress loss due to long term effects
Δf_{pT}	total prestress loss
θ	angle of inclination of diagonal compressive stresses (degrees)
ϕ	resistance factor
κ	multiplier for strand development length
τ	shear strength
σ	nominal strength
ρ_a	density of asphalt
ρ_c	density of concrete

This thesis reports values in US units (inch-pound) throughout. The following “hard” conversion factors have been used:

1 inch = 25.4 mm

1 ft = 0.3048 m

1 kip = 4.448 kN

1 ksi = 6.895 MPa

Reinforcing bar sizes are reported using the designation given in the appropriate reference. A bar designated using a “#” sign (e.g.: #4) refers to the standard inch-pound designation used in the United States where the number refers to the bar diameter in eighths of an inch.

ACKNOWLEDGEMENT

I am excited and pleased to express my gratitude to my graduate advisor, Dr. Kent A. Harries. During the past one year, his encouragement, guidance and patience deeply impressed me and are vital in forming this thesis. Also, his experience and insight are beneficial for developing my skills and understanding in both structural design and academic research. He spent exorbitant amount of time with me on this study and gave me lots of suggestions, which I must express my respect.

Besides, I would like to thank Mr. Teng Tong, the Ph.D. student of Dr. Qiang Yu. During the process, he improved my grammar and sentences a lot. Also his advices on how to analyze the data and draw the conclusions are really conducive. I really appreciated his assistance.

I would like to express my heartful thank to my professors, Dr. John Brigham, Dr. Qiang Yu, Dr. Morteza A.M. Torkamani and Dr. Piervincenzo Rizzo, leading me through my hard first semester here. I learnt far more than I expected here. I would also like to thank my friends, Mr. Mengzhe Gu, Mr. Ce Gao and Mr. Chunlin Pan for their support.

Finally, I send my deep gratitude to my parents and Mr. Wei Fu for their love, accompany, comfort, encouragement and support over the years. They support my dream of being an engineer and they are the anchor to me when I studied abroad. My most sincerely thank to all the ones above. Without you this thesis can never be finished.

1.0 INTRODUCTION

Pretensioned girders have gained large-scale acceptance and use because of their high quality and economic efficiency. However, some problems still exist and hinder the further application of longer and more heavily prestressed girders. The prestressing force in pretensioned girders can produce large stresses at both the top and bottom surfaces of the girders, especially near the ends of the girders where moments resulting from self-weight are minimal. Additionally, the transfer of large prestressing forces at girder ends can additionally lead to local cracking associated with bursting stresses or splitting. All these effects are compounded by the fact that prestressing force is introduced to the concrete at a very early age. Cracking can be mitigated by permitting greater concrete strength prior to prestressing transfer, but this is impractical and uneconomical. In practice, the magnitude of deleterious stresses can be reduced in three ways:

(1) Partial debonding (also known as blanketing or jacketing) a number of strands near the beam end;

(2) Harping some strands;

(3) Adding top strands.

Strands that can be harped are limited to those aligned with the member web(s), which may not be enough to sufficiently lower the stresses. Harped strands in relatively thin webs remain susceptible to splitting along their transfer length. Moreover, harping of 0.6 in. or 0.7 in.

strands poses challenges in terms of the capacity of hold-down devices and safety concerns, which are the main reasons why some fabricators will not harp strands.

The addition of top strands will increase girder cost and affects the overall stress state of the section, counteracting bottom strands in the critical midspan region. Top strands can be debonded over the midspan region and cut at midspan after transfer. This practice, however, complicates production and erection.

Compared to harping strands or adding top strands, partial debonding is easily accomplished using sheathing (flexible split-sheathing or rigid preformed tubes) or greasing. The prestressing force in partially debonded strands is transferred to the concrete at a distance from the end regions once bond is established. Thus, the total prestress force is introduced to the member gradually, reducing the stress concentrations and associated cracking at the beam ends. However, partial debonding of strands decreases the capacity of the longitudinal reinforcement particularly when cracks pass through the transfer length of debonded strands. If a large number of strands is debonded, the reduction of the longitudinal tension capacity could result in unacceptably reduced girder capacity issue near the supports. Excessive debonding can have other detrimental effects including the reduction of member flexure and shear capacity, and cracking associated with shear or load spreading.

1.1 SCOPE AND OBJECTIVE OF THESIS

Partially debonding straight prestressing strands near the ends of prestressed concrete bridge elements is an effective and economical way to address a number of early-age and serviceability issues. Since the use of higher strength concrete for carrying greater loads over longer spans

which requires greater prestressing forces is becoming more common, partial debonding becomes more critical to girder performance and to controlling end-region cracking.

Accordingly, the AASHTO *LRFD Specification* provides requirements for partially debonded strands. AASHTO requires that at a given section, the number of debonded strands should be limited to 25% of the total number of strands. The commentary notes that a larger percentage based on "successful past practice" may be considered. For example, Texas permits up to 75% debonding, while North Carolina allows up to 30%. Arizona, on the other hand, does not allow any partial debonding in I-girders. Currently, there is no consensus regarding the permitted level of debonding. Furthermore, no universally accepted guidelines are available for establishing the layout of debonded strands, release pattern of the bonded and partially debonded strands, the length of the debonding regions, or the staggering lengths of debonded strands, among other issues.

The proposed study focuses on partial debonding of straight strands used to control initial concrete stresses and cracking. The objective of the thesis is, therefore, to develop a unified approach to the design of partially debonded strand regions that addresses all aspects of the service and strength performance of the girder. This thesis will identify a number of AASHTO-prescribed performance and detailing issues that will be systematically studied using a purpose-written MATLAB program. The focus of the study is on quantifying the effects of partial debonding on the development of longitudinal forces in the prestressed reinforcement. Emphasis will be placed on the impact of partial debonding on the flexure and shear capacity of the member shear span (considering the increased forces carried by the longitudinal strands in the presence of shear). The goal of this thesis is to derive acceptable debonding ratios satisfying both

initial stress limits at prestress release and shear and flexural requirements at ultimate capacity for AASHTO girders (from Type III to Type IV) with different span lengths.

1.2 OUTLINE OF THESIS

This thesis addresses issues associated with the partially debonding of pretensioned girders, especially the determination of acceptable partial debonding ratios. Chapter 2 reviews bond mechanisms, calculations for transfer and development length and flexural and shear design for partial debonding, all based on AASHTO *LRFD Specification*. Chapter 3 presents the theoretical background and methodology of the MATLAB analyses conducted. Two series of 26 AASHTO Type III-VI girders with different debonding ratios are presented; one illustrative case is developed in a step-by-step manner. Chapter 4 presents a comparison of the results from the MATLAB program with those from *PCI Bridge Design Manual*. Additionally, the results are assessed against two criteria: the concrete tension stress limit of $0.24\sqrt{f_{ci}}$ and longitudinal tension capacity of the partially debonded strands, $A_{ps}f_{ps}$. Acceptable debonding ratios, ensuring that both criteria are satisfied, are obtained for the girders analyzed. Chapter 5 concludes the thesis and identifies issues that require for further study.

2.0 END REGION BEHAVIOR IN PRETENSIONED MEMBERS

2.1 INTRODUCTION

In pretensioned members, bond transfers force between the prestressing strands and surrounding concrete. At the ends of members, strand capacity is 'developed' through the transfer length and development length. These lengths provide the 'anchorage' for the initial prestress force and ultimate force in the strand, respectively. The relevant AASHTO *LRFD Specifications* (2010) regarding transfer and development lengths are presented in this chapter. The concept of and reasons for the practice of 'partial debonding', in addition to the benefits and drawbacks of the practice, are introduced. The role of the primary reinforcing steel in assuring the shear capacity of a member and the detrimental effect of partial debonding on this role are described.

2.2 BOND OF PRESTRESSING STRANDS

In the end-region of a pretensioned beam, the prestressing force is developed by bond between the prestressing strands and surrounding concrete as follows: First, the initial prestressing force is applied to the strands externally and tensile force is held. After the concrete is poured and the initial strength is obtained, the strands are cut or gradually released, allowing the tensile force – the 'initial prestressing force' – to transfer from the strand to the surrounding concrete as shown

schematically in Figure 2-1. Following the transfer, the force is maintained through bond between strand and the concrete in the end region near the strand termination. The region from end of the concrete (where concrete and strand stresses are necessarily zero) to where the entire initial prestress force is developed into the concrete is called 'transfer region' or 'transfer zone' (Figure 2-1). While the bond stress is highly nonlinear along the transfer length as shown in Figure 2-1, it is conventionally considered as a uniform average value making the prestressing strand and concrete stress variations linear as shown in Figure 2-1.

Loads applied subsequent to the transfer of the initial prestress force cause additional tension in the strand. This is also developed by bond although over a longer length referred to as the ‘development length’.

Bond between prestressing strand and concrete can be ascribed to three mechanisms (Briere et al. 2013): a) adhesion between the strand surface and the surrounding cementitious material; b) friction and the Hoyer effect (Hoyer 1939); and c) mechanical interlock between the helical-shaped seven-wire strands and the surrounding concrete. The Hoyer effect describes a wedge effect caused by the radial expansion of the strand following the release of the initial prestress force (Figure 2-2). This effect is analogous to and includes the Poisson expansion of the strand. The Hoyer effect results in friction along the strand length which enhances the mechanical interlock and makes the primary contribution to the transfer of initial prestressing force along the transfer length. Mechanical interlock dominates the development of stress caused by applied load distributed along the development length (Briere et al. 2013).

2.2.1 Transfer Length and Development Length

Making use of the uniform bond stress assumption, the AASHTO *LRFD Bridge Design Specification* (2010) defines strand development length in article 5.11.4.2:

$$l_d = \kappa(f_{ps} - \frac{2}{3} f_{pe})d_b \quad \text{(Eq. 2-1)}$$

Where f_{pe}= effective prestress; f_{ps} = the required stress in prestressing strands to be developed and d_b = the nominal strand diameter. The value of multiplier κ is 1.0 for pretensioned members for a depth smaller than 24 in. and 1.6 for members with a depth greater than 24 in. For members whose transfer length is not started from the end of the concrete (i.e. partially debonded strands), the multiplier κ is increased to 2.0, based on the recommendation from Kaar and Magura (1965) Equation 2-1 can be rewritten as:

$$l_d = l_{d1} + l_{d2} = \kappa \frac{f_{pe}}{3} d_b + \kappa(f_{ps} - f_{pe})d_b \quad \text{(Eq. 2-2)}$$

Where l_{d1} = the transfer length; l_{d2} = the flexural bond length. Typically, the transfer length is simplified as $60d_b$, corresponding to f_{pe} = 180 ksi which is a reasonable prestress estimation after losses. Thus, as shown in Figure 2-3, based on AASHTO *LRFD Specifications* (2010), the steel stress increases from zero to the effective prestressing stress (f_{pe}) through the transfer length ($60d_b$); stress due to subsequent applied loads is developed over the remaining flexural bond length. The development length is the sum of the transfer length and the flexural bond length.

2.3 PARTIAL DEBONDING

As described above, once concrete strength has achieved a minimum specified value the prestress force is transferred to the concrete. At prestress transfer eccentrically located strands introduce flexure into prestressed concrete girders. This flexure typically results in upward directed deflection, called camber, which will eventually be overcome by the application of structural loads. Camber results in tension at the top face of the member and compression at the bottom:

$$f_c = \frac{-P}{A} \pm \frac{Pe}{S} \quad \text{(Eq. 2-3)}$$

Where f_c is the concrete stress; P = the prestress force; e = the eccentricity of the prestress force and A and S are the section area and elastic modulus, respectively.

At prestress transfer, the tensile stress at the top surface of the concrete is only mitigated by the self-weight of the member:

$$f_c = \frac{-P}{A} + \frac{Pe}{S} + \frac{M_D}{S} \quad \text{(Eq. 2-4)}$$

Where M_D = the moment due to girder self-weight.

Near the girder ends, the value of M_D is negligible and the tensile stress often exceeds the cracking stress of the concrete – particularly since the concrete is typically several days old at the time of prestress transfer. The potential cracking is not only a structural concern but does affect durability, especially in bridge structures where the top surface of girders may eventually be subject to wetting or water ingress. For this reason, the AASHTO *LRFD Specifications* (2010) limits the allowable tensile stress at prestress transfer to $0.0948\sqrt{f_{ci}}$; where f_{ci} = the concrete compressive stress at prestress transfer measured in the unit of ksi. This is hard to meet and may

increases to $0.24\sqrt{f_{ci}}$, where mild reinforcement for controlling cracking is provided. Nonetheless, as to long girders requiring large amounts of prestressing strands, even the latter is difficult to meet.

There are two primary means of reducing the tensile stress at girder ends: a) harping strands to reduce the eccentricity and therefore the applied moment due to prestress force (Pe); b) debonding strands, resulting in reduced prestress force (P). Harping increases girder cost and is not practical in some cross sections.

Debonding involves 'blanketing' the strands near their ends so that they may not bond to the concrete. Once the M_D component is large enough to overcome the Pe component (Eq. 2-4) and maintain the value of $f_c \leq 0.24\sqrt{f_{ci}}$, the blanketing is terminated and bond is allowed to develop. In this case the transfer and development lengths of the blanketed strands does not initiate at the girder end but at the termination of the blanketing. This process is referred to as 'partial debonding' and is the focus of this work.

2.3.1 Bond Characteristics of Partially Debonded Strands

In general, for fully bonded strands (those bonded along their entire length from the end of the girder), the adequate embedment length is able to develop the tensile force demand in the strand along the entire length of a member. In the end region of a beam, large compressive forces will be caused by the prestress force and the vertical reaction force at support; these will also help to develop the strand anchorage. However, for partially debonded strands, the transfer length begins at the end of the debonded length. Thus, the anchorage zone of partially debonded strands is in a less beneficial condition compared with fully bonded strands. Additionally, the reduced embedment length of partially debonded strands may result in insufficient development to resist

eventual flexural and shear loads along the partially debonded region. Finally, based on tests of girders having partially debonded strands, Kaar and Magura (1965) put forward a recommendation that the value of κ in Eqs 2-1 and 2-2 for partially debonded strands should be increased to 2.0. This recommendation is adopted in the AASHTO *LRFD Specifications* (2010).

Burgueño and Sun (2011) indicated that different methods of sheathing used to debond strands have a significant influence on the transfer length of partially debonded strands. Based on their study, the transfer length of rigid sheathing was approximately 49% longer than that of flexible sheathing. The result indicated that flexible sheathing was not able to fully mitigate the bond mechanism associated with the expansion of prestressing strands (Hoyer effect) and bond transfer occurred over a shorter distance than expected. Thus, the concrete stresses in the debonded region may be higher than assumed in design and potentially cause cracking. Burgueño and Sun adopted a nonlinear FE model to calculate the stress transferred from the prestressing strands to the surrounding concrete and to evaluate end region damage when using flexible sheathing. They recommend using rigid sheathing to reduce end region cracks.

2.4 SPECIFICATIONS FOR PARTIALLY DEBONDED STRANDS

2.4.1 AASHTO LRFD Specifications (2010)

While both harping and debonding have been in use with relative success for some time, the cracking of beam ends continues to be a problem in the production of pretensioned concrete beams. Part of the reason for this lingering problem is that there are many influencing factors and the solution has been based on rough ad-hoc approaches or on simple elastic stress analyses.

AASHTO *LRFD Specifications* (2010) Article 5.11.4.3 provides the requirements for partially debonded strands as follows:

Length:

- The development length, which is measured from the end of the debonded zone, can be obtained from equation 5.11.4.2-1 multiplied by a factor of 2.0. (i.e. $\kappa = 2.0$)
- The length of debonding of any strand shall satisfy all limit states with consideration of the total developed resistance at any section being investigated.
- Exterior strands in each horizontal row shall be fully bonded.

Number:

- The number of partially debonded strands ***should*** not exceed 25% of the total number of strands.
- No more than 40% of strands in a horizontal row may be debonded.
- No more than the greater of 40% of the debonded strands or four strands shall have the debonding terminated at any section. This is referred to as 'staggering' the debonding terminations.

Details:

- Debonded strands shall be symmetrically distributed about the centerline of the member.
- Debonded length of pairs of strands that are symmetrically positioned about the centerline of the member shall be equal.

It is noted that all aspects of Articles 5.11.4.3 are in mandatory language ("shall") except the 25% of total strands limit ("should"); this implies that the *Specification* recommends a 25% limit but has an implied 40% limit based on the other requirements.

2.4.2 State Amended Specifications

State DOTs are permitted to amend AASHTO *LRFD Specifications* (2010). A selection of state-amended specifications for partially debonded strands are briefly summarized in Table 2-1. It is seen that practices vary and are occasionally contradictory (AZ and IN). Texas is known to permit up to 75% total debonding in its U-girders.

2.5 RELEVANT RESEARCH ON PARTIAL DEBONDING

2.5.1 Experimental Studies

Partial debonding is an effective way to reducing high concrete stresses in end regions of prestressed concrete members below AASHTO-acceptable limits. A number of past studies focused on eliminating end region cracking through the use of partial debonding (e.g. Ghosh and Fintel 1986, Oliva and Okumus 2010). These studies typically took the view of assessing the greatest level of partial debonding that is practical. Nonetheless, there remains a lack of consensus on the limits and applications of partial debonding. Observations, however, fall into two primary categories:

Firstly, partial debonding introduces a critical issue of reduced longitudinal flexural reinforcement, therefore span characteristics (i.e. the moment-to-shear ratio) will influence member behavior significantly (Kaar and Magura 1965, Rabbat et al. 1979, Russell and Burns 1993, Barnes et al. 1999). End region failures, including slip of prestressing strands and splitting are also observed which affect service, in addition to ultimate strength behaviour and capacity.

Secondly, partial debonding has little effect on shear capacity and can be neglected (Kaar and Magura, 1965; Abdalla et al. 1993; Barnes et al. 1999). Thus, the concrete (V_c) and transverse steel (V_s) components of shear capacity (described below in Section 2.6.1) are not affected. Although shear generates stress in the longitudinal strand, near the girder ends, the forces are mainly influenced by arching or direct strut action with the anchorage provided at the support (Ma et al. 1999). This observation does not address cases in which debonding is carried some ways into the girder span however.

2.5.2 Analytical Studies

The finite element method (FEM) is often adopted to model the global behavior of prestressed concrete members. But bond behavior and local effects in the end regions are complicated and numerous bond-slip models for strands and surrounding concrete are put forward. Baxi (2005) used finite element software (ABAQUS) to study the bond behaviour in both fully bonded and partially debonded strands, without considering concrete creep and shrinkage effects. In his simulation, the strand was modelled using truss elements and bond was modelled using nonlinear discrete spring elements.

Burgueño and Sun (2011) considered creep and shrinkage of concrete by replacing spring elements with a more realistic contact surface to model bond. They employed the damage-plasticity model for concrete and 3D solid elements for prestressing strands. Thus, the Hoyer effect could be simulated. However, mesh sizes were computationally unaffordable for analysis of full-scale members using 3D solid elements.

2.6 SHEAR RESISTANCE AND BEHAVIOR OF PRESTRESSED GIRDERS

The AASHTO *LRFD Specifications* (2010) provides two methods to calculate shear resistance of prestressed concrete elements: (1) the General Procedure in Article 5.8.3.4.2, and (2) the Simplified Procedure in Article 5.8.3.4.3. These two methods have similar requirements for the design of minimum reinforcement, maximum shear limits, and for accounting for the effect of the vertical component of prestressing, but they have different methodologies for calculating the concrete and steel components of shear resistance.

2.6.1 Nominal Shear Resistance

Article 5.8.3.3 provides the equation for the nominal shear resistance, V_n:

$$V_n = \min(V_c + V_s + V_p, 0.25 f_c' b_v d_v + V_p) \quad \text{(Eq. 2-5)}$$

In which

$$V_c = 0.0316\beta\sqrt{f_c'} b_v d_v \text{ (ksi)} \quad \text{(Eq. 2-6)}$$

$$V_s = \frac{A_v f_y d_v (\cot\theta + \cot a)}{s} \quad \text{(Eq. 2-7)}$$

Where V_c = the concrete contribution to shear resistance; f_c' = concrete compressive strength; b_v and d_v are section web breadth and depth, respectively; V_s = the shear resistance provided by shear reinforcement having a yield capacity of f_y, area of A_v and spacing of s; V_p is the vertical component of the effective prestressing force. In section having no harped strands, $V_p = 0$. The upper limit, $V_c + V_s \leq 0.25 f_c' b_v d_v$ is intended to control the diagonal compressive stresses and is based on the maximum diagonal tension strain in the member web. The values of the β and θ are

determined using the Modified Compression Field Theory (MCFT) as adopted in Article 5.8.3.4.2.

2.6.2 Longitudinal Reinforcement

In a flexural member, shear will cause a tensile force in the longitudinal reinforcement in addition to that required to resist the flexure. Diagonal cracks usually occur near the support and the free body diagram can be drawn as shown in Figure 2-4. Summing moments about the compressive resultant force (point O), the additional tensile force in the longitudinal reinforcement, T_v, can be calculated as:

$$\sum M_O = T_v d_v + V_s(0.5 d_v \cot\theta) - \left|\frac{V_u}{\phi_y} - V_p\right| d_v \cot\theta = 0 \qquad \text{(Eq. 2-8)}$$

$$T_v = \left(\left|\frac{V_u}{\phi_y} - V_p\right| - 0.5V_s\right)\cot\theta \qquad \text{(Eq. 2-9)}$$

As the inclination of the diagonal crack, θ, becomes smaller (flatter) the additional tensile force T_v will increase. Article 5.8.3.5 prescribes that half of the applied factored axial tension load, N_u, is resisted by the longitudinal reinforcement. Considering the effects of flexure, shear and axial load, the total tensile force in the primary longitudinal reinforcing steel is:

$$T = \frac{|M_u|}{d_v\phi_f} + 0.5\frac{N_u}{\phi_v} + \left(\left|\frac{V_u}{\phi_v} - V_p\right| - 0.5V_s\right)\cot\theta \qquad \text{(Eq. 2-10)}$$

Adequate longitudinal reinforcement, including both prestressing strands and non-prestressed bars, must provide enough tensile force to resist the total tensile force:

$$A_{ps} f_{ps} + A_s f_y \geq T = \frac{|M_u|}{d_v\phi_f} + 0.5\frac{N_u}{\phi_v} + \left(\left|\frac{V_u}{\phi_v} - V_p\right| - 0.5V_s\right)\cot\theta \qquad \text{(Eq. 2-11)}$$

AASHTO provides that in the critical region for shear extending from the inside edge of the bearing area of simple end supports to the section of critical shear, the longitudinal reinforcement on the flexural tension side of the member shall satisfy:

$$A_{ps} f_{ps} + A_s f_y \geq \left(\left|\frac{V_u}{\phi_v} - V_p\right| - 0.5V_s\right)\cot\theta \qquad \text{(Eq. 2-12)}$$

Neglecting flexure and axial effects in this region reflect the expected beneficial effects of arching action in this region as described by Ma et al. (1999).

Equations 2-11 and 2-12 clearly indicate that the longitudinal reinforcement is used to resist shear. Moreover, equation 2-12 should consider the possibility that tensile stress in the longitudinal reinforcement may not be fully developed at the critical section; that is f_{pu} may not be fully developed at this section and thus $f_{ps} < f_{pu}$. Therefore the available strands capacity must be determined based on the available development length. Partially debonded strands in this region clearly do not contribute to the resistance of the tension force T.

For a simple support beam with only prestressing strands, Equation 2-11 can be rewritten as $(A_{ps}f_{ps})/T \geq 1$ and can be used to determine whether available tensile capacity can be developed in prestressing strands or not. If the value of $(A_{ps}f_{ps})/T$ is less than 1 then the required tensile stress cannot be fully developed and additional reinforcement is required.

Table 1. Selection of state-amended requirements for partially debonded strands

State	Total strands permitted to be debonded	Strands in one row permitted to be debonded	Staggering cut-offs	Other
AASHTO	25%	40%	40% or 4 strands	
PA (2000)	25%	40%	40% or 4 strands	additional 50% within 6 in. of beam end and 25% within 36 in. permitted for crack control
NY (2006)	25%	40% but spacing must exceed 4 in.	at least 24 in. spacing	not permitted in members having d < 15 in.
OH (2007)	25% mandatory for I-girders	40%	40% or 4 strands	maximum debonding length must be less than 0.16L-40 in. and 50% of debonded strands must be only half this length
AZ (2011)	25%	40%	40% or 4 strands	debonding not permitted for I-girders
IN (2011)	25% 50% for I-girders	40%	40% or 4 strands	
NE (2011)	increase of 20% beyond AASHTO limits permitted with engineer's permission			
NC (2011)	30% (25% 'preferred')	40%	40% or 4 strands	

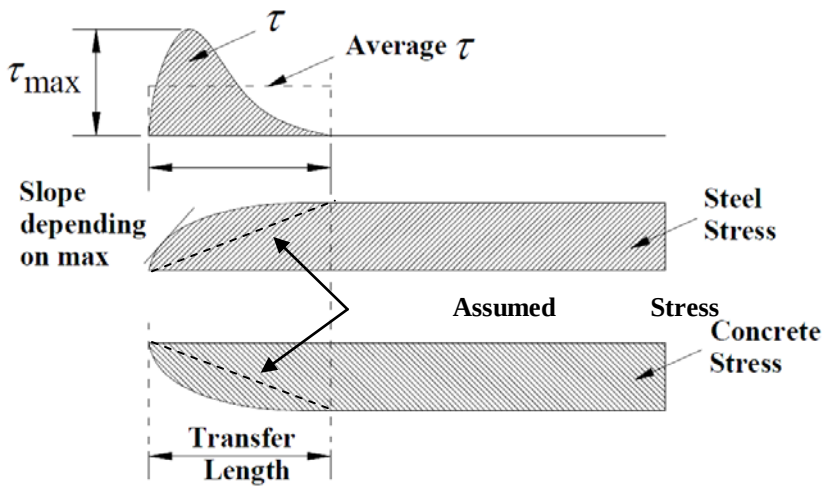

Figure 1. Bond stress distribution and transfer length (adapted from Leonhardt 1964)

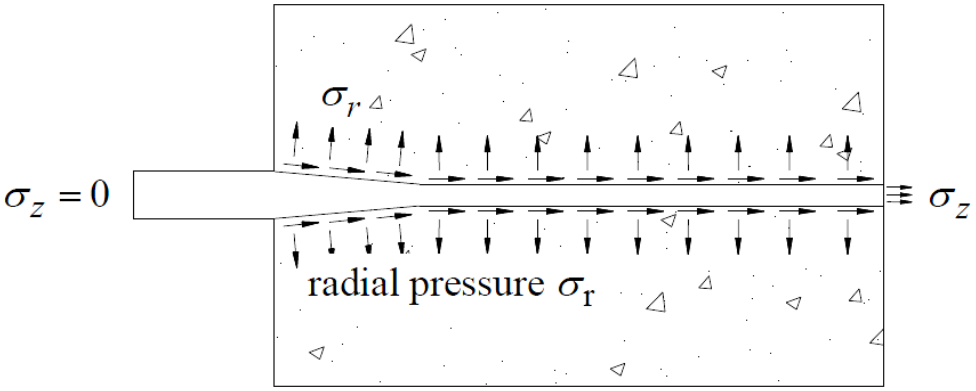

Figure 2. Schematic representation of the Hoyer effect (adapted from Burgueño 2011)

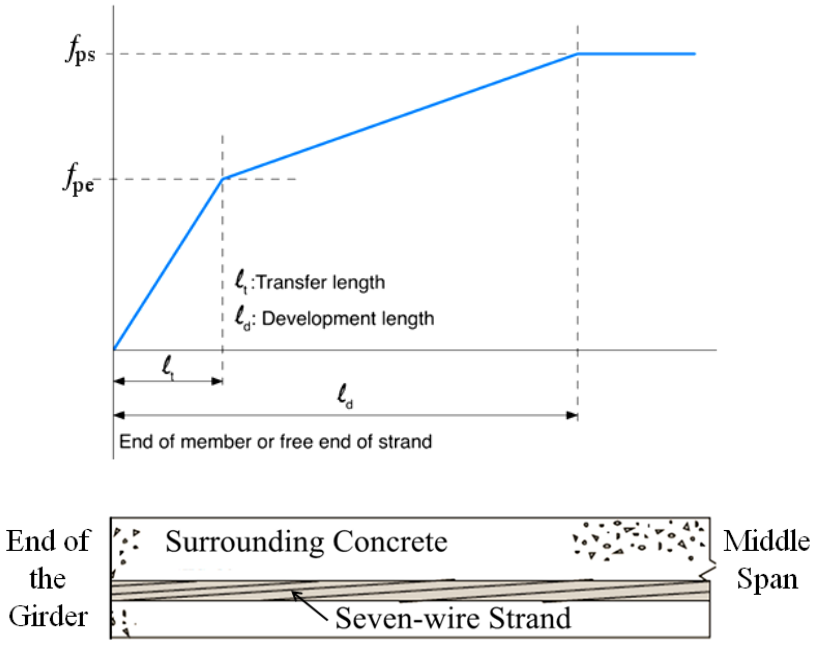

Figure 3. Transfer and development lengths based on uniform bond assumptions of AASHTO LRFD Specifications (adapted from Kasan 2012)

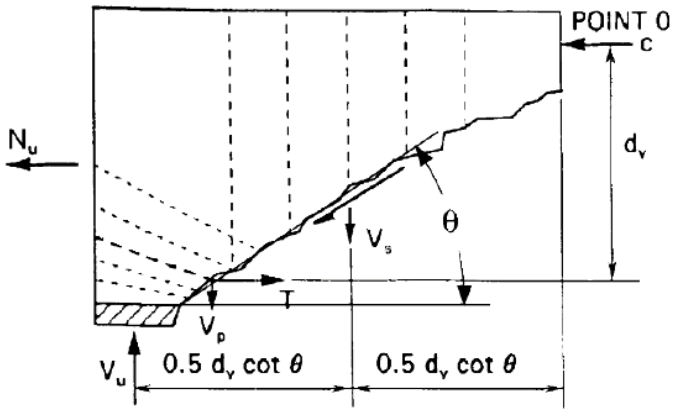

Figure 4. Free body diagram of forces after diagonal crack forms (AASHTO Specifications Article C5.8.3.5)

3.0 PARTIAL DEBONDING EFFECTS

3.1 INTRODUCTION

The prestressing force can produce large stresses in pretensioned girders. Near the ends of the girders, span effects (i.e. dead load moment) are minimal; but the transfer of large prestressing forces, applied with an eccentricity to the section, can result in cracking associated with the induced flexure at the top surface of the girder. Additionally, prestressing forces can cause local cracking, associated with spreading of prestressed forces in bulb-flanges or due to the Hoyer effect near the strand ends, or splitting, associated with transfer of the strand force through bond along the transfer length. These effects are made worse by the fact that prestress transfer occurs at a concrete age as early as 18-24 hours, before the tensile resistance of the concrete is well established. In order to reduce end region cracking, prestress transfer can be delayed in order to increase concrete strength; otherwise the prestress forces must be reduced. The former is not considered economical or practical in the prestressed concrete industry that relies on 24 hour casting cycles. Reduction of detrimental forces can be implemented in three primary ways: 1) partial debonding of strands (the focus of this study); 2) harping strands; and/or 3) adding top strands. Harping is not an available option for some kinds of girders (i.e. box girders) and is expensive, awkward and introduces additional concerns, including factory safety concerns, associated with strand hold down requirements. Additionally, harping may not entirely alleviate

issues associated with splitting cracks since the harped strands are often located in the very thin web elements of bulb-flanged girders.. Adding top strands – which reduces the negative moment at the girder ends and thus mitigates top surface cracking – increases costs and influences stress states along the entire girder length. Partial debonding and severing of top strands in the mid-span region has been used to reduce the effect of top strands over the entire span, although these solutions are also costly and introduce new concerns of their own.

Compared with the other two methods, partial debonding of straight strands is easily accomplished with and has minimal cost. In partially debonded strands, the strands are 'blanketed' in order to transfer no stress to the concrete over a distance from the end of the girder. Stress is only transferred once the blanketing is terminated and bond is re-established. In this way, the large prestressing force is introduced gradually into the girder, decreases the concentrated stress transfer at the end of the girder. Partial debonding can, in many instances, effectively control or eliminate local cracking.

However, partial debonding reduces the longitudinal capacity of the girder over the region of partial debonding and over the extended development length of the debonded strands. This is particularly critical where there is a shear crack passing through this region (Barnes et al., 1999). At the end of the girder, over the support and often beyond the 'critical section for shear' (usually taken as a distance of one half the girder depth from the face of the support), the largest number of strands is debonded and the longitudinal tension capacity is most affected. This is the very region where longitudinal stress in the primary reinforcing steel is increased by the effects of shear, as described previously in Section 2.6.1.

AASHTO provides both requirements and recommendations for partial debonding – these are described in Section 2.4.1. Nevertheless, as noted in Section 2.4.2, there is no consensus on details partial debonding, particularly the maximum debonding permitted.

3.1.1 Objective

If a unified approach to partial debonding practice is to be developed, all aspects of the strength and service performance of the girder must be considered. Partial debonding has a dominant effect on flexural capacity near the ends of a girder and may also impact shear performance as partial debonding termination represents a stress-raiser of sorts in the high-shear regions of a pretensioned girder. In this work, analytical studies are developed to quantify effects of partial debonding with respect to these effects and in the development of longitudinal forces in the prestressing strands.

In this work, extensive study of strand debonding in AASHTO Type III-VI girders is carried out. Required debonding ratios – defined as the total number of partially debonded strands to the total number of strands in the section – are found for various girder and bridge geometries to satisfy the AASHTO compression and tension stress limits for concrete in pretensioned members described in AASHTO *Specifications* Articles 5.9.4.1.1 and 5.9.4.1.2:

Concrete compression stress limit: $f_c \leq 0.60 f_{ci}$; and

Concrete tension stress limit: $f_c \leq 0.24\sqrt{f_{ci}}$ (ksi)

Where f_{ci} = concrete strength at the time of prestressing force transfer (absolute values of stress are assumed in both cases). The compression limit primarily affects the greatest number of strands that may be placed in a section. The tension limit, usually critical at the girder ends, where span effects are negligible, affects the required amount of partial debonding.

Having established the required partial debonding to meet concrete stress limits at prestress transfer, the girder ultimate flexural and shear capacity is then considered. In Section 2.5.1.2, for a simply support beam, Equation 2-10, defining the total stress carried by the longitudinal reinforcing steel, must be satisfied at all locations along the span. Between the supports and the critical section for shear, AASHTO permits the designer to consider only shear in determining the stress which the longitudinal reinforcement must resist, as shown in Equation 2.12. Assuming no mild reinforcement component, both of these equations are simplified by the capacity check:

$$A_{ps} f_{ps} / T \geq 1 \qquad \text{(Eq. 3-1)}$$

Where T is described by Equation 2.10 or 2.12 depending on the location being considered in the span. If the value of $(A_{ps}f_{ps})/T$ is less than 1, the required tensile stress cannot be developed by the available reinforcement. This may occur 1) if too many strands are debonded; i.e.: A_{ps} is too small; or 2) the strands that are present are not fully developed; i.e.: $f_{ps} < f_{pu}$.

3.1.2 Scope

The premise of this work is that partial debonding is an established practice for pretensioned girders. The work develops a methodology establishing an appropriate maximum debonding ratio that addresses all aspects of girder design. Two series of 26 AASHTO Type III-VI girders with different debonding ratios are analysed using the AASHTO design procedures (a MATLAB worksheet for representative Case B29 is provided in Appendix A; a summary of calculation for Case B29 is provided in Appendix B). All analysis is based on AASHTO *LRFD Specification* requirements. Results from the MATLAB analysis are compared initial design values provided in the *PCI Bridge Design Manual* (2011) in order to validate the model. Critical concrete tensile

stress and longitudinal tension capacity are computed to establish the efficacy of the partial debonding provided.

3.2 PROTOTYPE GIRDERS

3.2.1 Girder Selection

In this study, AASHTO Type III, IV, V and VI girders are considered. Girders are divided into two series: Series A and Series B.

Series A considers 14 girders. In this series the span length and total number of strands is constant and the girder size is varied. The cases considered are reported in Table 3-1.

Series B considers 12 Type IV girders with the total number of strands held constant, while the girder length and spacing is varied. The cases considered are reported in Table 3-2.

Girder dimensions are given in Figure 3-1 and Table 3-3. Gross section properties of the girders (without slabs) are given in Table 3-4. The maximum permitted strand arrangement is shown in Figure 3-2.

All prototype girders are designed based on the procedure laid out in Appendix A5 of the AASHTO *LRFD Specification*. All are assumed to be interior girders of un-skewed multiple-girder bridges having at least five girders. Based on this, different combinations of span length, L, and girder spacing, S, result in the same required girder capacity; hence the groupings by number of strands, N, in Tables 3-1 and 3-2. Solid slabs having thickness, t_s, given in Table 3-5 span between the girders. The effective width of the slabs – for determining girder resistance – is

taken as that described by AASHTO: the least of 1) 25% of the span length; 2) 24 times the slab thickness (Table 3-5); or 3) the girder center-to-center spacing, S.

All girders are simply supported over the span shown in Tables 3-1 or 3-2. Bearing support length is 10 in. in every case and the girders are supported over the full bottom flange width (dimension B2 in Figure 3-1 and Table 3-3). All girders were provided with #4 stirrups as shear reinforcement; these are spaced at 24 in. over the remainder of the span.

3.2.2 Partial Debonding

Four levels of partial debonding are considered for each prototype girder: no partial debonding and approximately 25%, 50% and 75% partial debonding. Actual debonding ratios, dr, vary slightly since only an even number of strands may be debonded while still respecting symmetry in the girder. In all cases, debonding is incrementally applied over three, 3 ft long segments extending from the girder ends as shown in Figure 3-3. The maximum debonding occurs over the support location (from the end of the beam to 3 feet) and all strands are fully bonded at 9 ft. Details of each prototype beam and debonding arrangement are given in Tables 3-6 and 3-7 for Series A and B, respectively. In these tables, the maximum debonding ratio, dr, is given and the ***bonded*** strand arrangement is given. Only four rows of strands are considered (Figure 3-2), these are labelled R1 to R4 from the bottom-up. Selected debonding patterns, preferentially maintained strands in R1 and R2; in some cases debonding 100% of strands in R3 and R4. The total number of strands in each section and their arrangement are given in the final columns of Tables 3-6 and 3-7 as the strand arrangement from 9 ft to mid-span. All details are symmetric about mid-span.

3.2.3 Assumed Material Properties

3.2.3.1 Prestressing Steel

All girders are reinforced with 0.6 in. diameter low-relaxation seven wire strand. This strand has an area, A_{ps} = 0.215 in^2 and an ultimate strength of f_{pu} = 270 ksi. The strand modulus of elasticity is E_p = 28500 ksi. The initial prestressing force is $f_{pi} = 0.75f_{pu}$ = 203 ksi. Losses are transfer are assumed to be $0.11f_{pu}$ = 29.4 ksi, resulting an effective prestress force at transfer of $f_{pe} = 0.64f_{pu}$ = 173.1 ksi. When considering ultimate capacity, the effective long term prestress force is assumed to be $0.56f_{pu}$ = 151 ksi.

3.2.3.2 Concrete

The assumed 28-day compressive strength of the girders is $f_c' = 8$ ksi, while that of the additional slab (Table 3-5) is $f_c' = 4$ ksi. The girder strength at prestress transfer is assumed to f_{ci} = 6.8 ksi. Thus the compressive stress limit at prestress transfer is $f_c < 0.60f_{ci}$ = 4.1 ksi. The concrete tensile stress limit is $f_c < 0.24\sqrt{f_{ci}}$ = 0.63 ksi. The concrete strength at prestress transfer, although it is that used to establish initial design details in the *PCI Bridge Design Manual* may be higher than is seen in practice. A value of $0.6f_c$, equal to 4.8 ksi in this case, is more typical.

3.2.4 Applied Loads

3.2.4.1 At Prestress Transfer

At prestress transfer, the girders are assumed to be simply supported over their span L and have attained a concrete strength of f_{ci} = 6.8 ksi. Only the self-weight of the girder, given in Table 3-4, is applied as a uniformly distributed load. The ratio of allowed tension stress to the maximum

concrete tension stress is determined at the face of the support and at the critical section for shear, d/2 from the face of the support, where d = the girder depth:

$0.24\sqrt{f_{ci}}/f_t$ (Eq. 3-2)

The value of the tension stress at the top surface of the section is found from Eq. 2-4. For these calculations, a load factor of unity is used.

3.2.4.2 STENGTH I Load Condition

In order to assess the efficacy of the partially debonded strands to resist ultimate loads, the tensile stresses developed in the strand (Eqs. 2-10 and 2-12) are determined and the capacity-to-demand ratio is found:

$A_{ps}f_{ps}/T$ (Eq. 3-3)

Where f_{ps} is determined as the stress which may be developed in the strand at the location of interest. That is, $f_{ps} = 0$ for strands that are partially debonded. Additionally, once bonded, the transfer and development lengths of these strands, calculated using Eq. 2-2 are determined applying the factor $\kappa = 2$.

Only the STRENGTH I load combination (AASHTO Article 3.5 and 3.6) is considered:

$1.25DC + 1.5DW + 1.75(LL + IM)$ (Eq. 3-4)

Where DC is the weight of components, including:

the girder self weight (Table 3-4)

the self weight of the concrete slab ($\rho_c = 150$ pcf)

DW is the weight of the wearing surface; in these analyses, a 3 in. asphalt ($\rho_a = 125$ pcf) wearing surface is assumed.

LL is the AASHTO-specified HL-93 live load combination specified as the greater effect of 1) HL-93 design truck load + 640 plf lane load; or 2) design tandem load + 640 plf design lane

load. The spans, in all cases are sufficiently long that the HL-93 truck, shown in Figure 3-4a, governs design for moment. The location of the HL-93 vehicle for determining shear capacity is shown in Figure 3-4b.

IM is the dynamic load allowance taken as 0.33LL; thus the final term in Eq. 3-4 becomes 1.75(LL + 0.33LL) = 2.33LL.

The multiple presence factor is taken as 1.0, assuming that two lanes are loaded and the distribution factors for moment and shear are calculated accordingly (AASHTO Article 4.6.2.2). The bridges are assumed to be unskewed, therefore the skew correction factor is 1.0.

3.3 REPRESENTATIVE PROTOTYPE EXAMPLE

In order to demonstrate the analysis conducted using the MATLAB program, a representative example – Case B29 in Table 3-7 – is presented in detail in the this section. Complete calculations are presented in Appendix B. The prototype is a 105-foot long AASHTO Type IV girder having 26-0.6-in., 270-ksi straight strands arranged in three rows having 10, 8 and 8 strands, respectively, as shown in Figure 3-3.

Twelve of the 26 strands (46%) were debonded over the initial 3 feet, eight strands (31%) were debonded to 6 feet, and four strands (15%) were debonded to 9 feet. From 9 feet to the mid-span all 26 strands are fully bonded. The maximum debonding ratio is 0.46 for this girder. The girder section and elevation are shown in Figure 3-3. Based on AASHTO *Specifications*, the transfer length (see Section 2.2.1) is $l_t = 1.6(60d_b) = 58$ in. for the fully bonded strands and $l_t = 2.0(60d_b) = 72$ in. for the partially debonded strands as shown in Figure 3-6. Similarly, the

development length for the partially debonded strands is $2.0l_d$ = 175 in. and $1.6l_d$ =140 in. for the fully bonded strands (Figure 3-5).

The strand stress immediately after transfer is 173 ksi. The prestress transfer results in the beam 'hogging' and concrete tension forces generated along the top surface. These are only mitigated by the girder self-weight. If no partial debonding were present, the concrete tensile stress near the support (calculated using Eq. 2-3) significantly exceeds the concrete tensile stress limit:

$$f_c = \frac{-P}{A} + \frac{Pe}{S} \le 0.24\sqrt{f_{ci}} = 0.24\sqrt{6.8} = 0.63ksi \qquad \text{(Eq. 3-5)}$$

$$f_c = \frac{-(26\times 0.215\times 173)}{789} + \frac{(10\times 0.215\times 173)\times(y_b - 2)}{8908} + \frac{(8\times 0.215\times 173)\times(y_b - 4)}{8908}$$
$$+ \frac{(8\times 0.215\times 173)\times(y_b - 6)}{8908} = 1.04ksi > 0.63ksi.....exceeds$$

Where y_b = 24.73 in. for AASHTO Type IV girders (Table 3-4) and the individual layers of 10, 8 and 8 strands are spaced at 2 in. (i.e.: e = y_b – 2 for lowest row of strands, etc.). As demonstrated by Equation 3-5, partial debonding is required. In this case, the 46% debonding provided successfully reduced the tensile stresses below the prescribed limit as shown in Figure 3-6. In this case, the 26 strand arrangement does not result in concrete compressive stress exceeding the permitted limit of $0.6f_{ci}$ – this is also shown in Figure 3-6.

Under the STRENGTH I load combination the maximum moment and shear effects are generated. Figure 3-7a shows the prestressing strand capacity ratio given by Eq. 3-1 along the girder span. It is seen that this ratio exceeds unity – indicating adequate capacity – from just beyond the face of the support. At the critical section, the ratio is 2.04. AASHTO *Specifications* (and common design practice) neglects shear-induced effects in the region between the face of the support and the critical section for shear; thus the strand capacity is adequate for Case B29.

Figure 3-7b shows the shear capacity and demand along the entire girder. Due to the length of the girder, the shear demand is not significant and remains comfortably below the shear capacity provided by the girder.

Table 2. Series A

Girder Length (ft)	No. of Strands in mid-span	Girder Type	Girder Spacing (ft)
L	N		S
50	12	III	10
		IV	12
		V	12
70	16	III	8
		IV	10
		V	10
		VI	12
100	28	III	6
		IV	8
		V	10
		VI	12
125	40	IV	6
		V	8
		VI	10

Table 3. Series B

Girder Length (ft)	No. of Strands in mid-span	Girder Type	Girder Spacing (ft)
L	N		S
65	12	IV	6
60			8
55			10
50			12
105	26		6
95			8
90			10
85			12
120	38		6
115			8
105			10
100			12

Table 4. Dimensions (in.) shown in Figure 3-1 (PCI Bridge Design Manual, 2011)

Girder Type	D1	D2	D3	D4	D5	D6	B1	B2	B3	B4	B5	B6
III	45.0	7.0	0.0	4.5	7.5	7.0	16.0	22.0	7.0	4.5	0.0	7.5
IV	54.0	8.0	0.0	6.0	9.0	8.0	20.0	26.0	8.0	6.0	0.0	9.0
V	63.0	5.0	3.0	4.0	10.0	8.0	42.0	28.0	8.0	4.0	13.0	10.0
VI	72.0	5.0	3.0	4.0	10.0	8.0	42.0	28.0	8.0	4.0	13.0	10.0

Table 5. Gross section properties (PCI Bridge Design Manual, 2011)

Girder Type	Section Area $in.^2$	Distance from Neutral Axis to Soffit) in.	Moment of Inertia $in.^4$	Girder Self Weight kip/ft
	A	yb	I	w
III	560	20.27	125,390	0.583
IV	789	24.73	260,730	0.822
V	1013	31.96	521,180	1.055
VI	1085	36.38	733,320	1.130

Table 6. Slab thickness

Girder Spacing (ft)	Thickness of Slab (in.)
S	t_s
6	8
8	8
10	8.5
12	9

Table 7. Debonding arrangements for Series A

Case ID	AASHTO Type	Span Length	Spacing	Total strands	Max. debond ratio	Bonded Strands in each row (R) from the bottom of the girder															
						0' to 3'				3' to 6'				6' to 9'				9' to L/2			
		L (ft)	S (ft)	N	dr	R1	R2	R3	R4	R1	R2	R3	R4	R1	R2	R3	R4	R1	R2	R3	R4
A1	III	70	8	16	0.00	8	8	0	0	8	8	0	0	8	8	0	0	8	8	0	0
A2	IV	70	10	16	0.00	8	8	0	0	8	8	0	0	8	8	0	0	8	8	0	0
A3	V	70	10	16	0.00	8	8	0	0	8	8	0	0	8	8	0	0	8	8	0	0
A4	VI	70	12	16	0.00	8	8	0	0	8	8	0	0	8	8	0	0	8	8	0	0
A5	III	100	6	28	0.00	10	10	8	0	10	10	8	0	10	10	8	0	10	10	8	0
A6	IV	100	8	28	0.00	10	10	8	0	10	10	8	0	10	10	8	0	10	10	8	0
A7	V	100	10	28	0.00	10	10	8	0	10	10	8	0	10	10	8	0	10	10	8	0
A8	VI	100	12	28	0.00	10	10	8	0	10	10	8	0	10	10	8	0	10	10	8	0
A9	III	50	10	12	0.00	8	4	0	0	8	4	0	0	8	4	0	0	8	4	0	0
A10	IV	50	12	12	0.00	8	4	0	0	8	4	0	0	8	4	0	0	8	4	0	0
A11	V	50	12	12	0.00	8	4	0	0	8	4	0	0	8	4	0	0	8	4	0	0
A12	IV	125	6	40	0.00	12	12	12	4	12	12	12	4	12	12	12	4	12	12	12	4
A13	V	125	8	40	0.00	12	12	12	4	12	12	12	4	12	12	12	4	12	12	12	4
A14	VI	125	10	40	0.00	12	12	12	4	12	12	12	4	12	12	12	4	12	12	12	4
A15	III	70	8	16	0.25	6	6	0	0	8	6	0	0	8	8	0	0	8	8	0	0
A16	IV	70	10	16	0.25	6	6	0	0	8	6	0	0	8	8	0	0	8	8	0	0
A17	V	70	10	16	0.25	6	6	0	0	8	6	0	0	8	8	0	0	8	8	0	0
A18	VI	70	12	16	0.25	6	6	0	0	8	6	0	0	8	8	0	0	8	8	0	0
A19	III	100	6	28	0.21	8	8	6	0	10	8	6	0	10	10	6	0	10	10	8	0
A20	IV	100	8	28	0.21	8	8	6	0	10	8	6	0	10	10	6	0	10	10	8	0
A21	V	100	10	28	0.21	8	8	6	0	10	8	6	0	10	10	6	0	10	10	8	0
A22	VI	100	12	28	0.21	8	8	6	0	10	8	6	0	10	10	6	0	10	10	8	0

Table 7. (continued)

Case ID	AASHTO Type	Span Length	Spacing	Total strands	Max. debond ratio	Bonded Strands in each row (R) from the bottom of the girder															
						0' to 3'				3' to 6'				6' to 9'				9' to L/2			
		L (ft)	S (ft)	N	dr	R1	R2	R3	R4	R1	R2	R3	R4	R1	R2	R3	R4	R1	R2	R3	R4
A23	III	50	10	12	0.17	6	4	0	0	8	4	0	0	8	4	0	0	8	4	0	0
A24	IV	50	12	12	0.17	6	4	0	0	8	4	0	0	8	4	0	0	8	4	0	0
A25	V	50	12	12	0.17	6	4	0	0	8	4	0	0	8	4	0	0	8	4	0	0
A26	IV	125	6	40	0.25	10	10	10	0	12	12	10	0	12	12	12	2	12	12	12	4
A27	V	125	8	40	0.25	10	10	10	0	12	12	10	0	12	12	12	2	12	12	12	4
A28	VI	125	10	40	0.25	10	10	10	0	12	12	10	0	12	12	12	2	12	12	12	4
A29	III	70	8	16	0.50	4	4	0	0	6	6	0	0	8	8	0	0	8	8	0	0
A30	IV	70	10	16	0.50	4	4	0	0	6	6	0	0	8	8	0	0	8	8	0	0
A31	V	70	10	16	0.50	4	4	0	0	6	6	0	0	8	8	0	0	8	8	0	0
A32	VI	70	12	16	0.50	4	4	0	0	6	6	0	0	8	8	0	0	8	8	0	0
A33	III	100	6	28	0.50	6	6	2	0	8	8	2	0	10	10	4	0	10	10	8	0
A34	IV	100	8	28	0.50	6	6	2	0	8	8	2	0	10	10	4	0	10	10	8	0
A35	V	100	10	28	0.50	6	6	2	0	8	8	2	0	10	10	4	0	10	10	8	0
A36	VI	100	12	28	0.50	6	6	2	0	8	8	2	0	10	10	4	0	10	10	8	0
A37	III	50	10	12	0.50	4	2	0	0	6	2	0	0	8	4	0	0	8	4	0	0
A38	IV	50	12	12	0.50	4	2	0	0	6	2	0	0	8	4	0	0	8	4	0	0
A39	V	50	12	12	0.50	4	2	0	0	6	2	0	0	8	4	0	0	8	4	0	0
A40	IV	125	6	40	0.50	8	8	4	0	12	10	4	0	12	12	8	2	12	12	12	4
A41	V	125	8	40	0.50	8	8	4	0	12	10	4	0	12	12	8	2	12	12	12	4
A42	VI	125	10	40	0.50	8	8	4	0	12	10	4	0	12	12	8	2	12	12	12	4
A43	III	70	8	16	0.75	2	2	0	0	4	4	0	0	6	6	0	0	8	8	0	0
A44	IV	70	10	16	0.75	2	2	0	0	4	4	0	0	6	6	0	0	8	8	0	0

Table 7. (continued)

Case ID	AASHTO Type	Span Length	Spacing	Total strands	Max. debond ratio	Bonded Strands in each row (R) from the bottom of the girder															
						0' to 3'				3' to 6'				6' to 9'				9' to L/2			
		L (ft)	S (ft)	N	dr	R1	R2	R3	R4	R1	R2	R3	R4	R1	R2	R3	R4	R1	R2	R3	R4
A47	III	100	6	28	0.71	4	4	0	0	6	6	2	0	8	8	4	0	10	10	8	0
A48	IV	100	8	28	0.71	4	4	0	0	6	6	2	0	8	8	4	0	10	10	8	0
A49	V	100	10	28	0.71	4	4	0	0	6	6	2	0	8	8	4	0	10	10	8	0
A50	VI	100	12	28	0.71	4	4	0	0	6	6	2	0	8	8	4	0	10	10	8	0
A51	III	50	10	12	0.67	4	0	0	0	6	2	0	0	8	2	0	0	8	4	0	0
A52	IV	50	12	12	0.67	4	0	0	0	6	2	0	0	8	2	0	0	8	4	0	0
A53	V	50	12	12	0.67	4	0	0	0	6	2	0	0	8	2	0	0	8	4	0	0
A54	IV	125	6	40	0.70	6	6	0	0	10	8	4	0	12	10	8	2	12	12	12	4
A55	V	125	8	40	0.70	6	6	0	0	10	8	4	0	12	10	8	2	12	12	12	4
A56	VI	125	10	40	0.70	6	6	0	0	10	8	4	0	12	10	8	2	12	12	12	4

Table 8. Debonding arrangements for Series B

Case ID	AASHTO Type	Span Length	Spacing	Total strands	Max. debond ratio	Bonded Strands in each row (R) from the bottom of the girder															
						0' to 3'				3' to 6'				6' to 9'				9' to L/2			
		L (ft)	S (ft)	N	dr	R1	R2	R3	R4	R1	R2	R3	R4	R1	R2	R3	R4	R1	R2	R3	R4
B1	IV	65	6	12	0.00	8	4	0	0	8	4	0	0	8	4	0	0	8	4	0	0
B2	IV	60	8	12	0.00	8	4	0	0	8	4	0	0	8	4	0	0	8	4	0	0
B3	IV	55	10	12	0.00	8	4	0	0	8	4	0	0	8	4	0	0	8	4	0	0
B4	IV	50	12	12	0.00	8	4	0	0	8	4	0	0	8	4	0	0	8	4	0	0
B5	IV	105	6	26	0.00	10	8	8	0	10	8	8	0	10	8	8	0	10	8	8	0
B6	IV	95	8	26	0.00	10	8	8	0	10	8	8	0	10	8	8	0	10	8	8	0
B7	IV	90	10	26	0.00	10	8	8	0	10	8	8	0	10	8	8	0	10	8	8	0
B8	IV	85	12	26	0.00	10	8	8	0	10	8	8	0	10	8	8	0	10	8	8	0
B9	IV	120	6	38	0.00	12	12	10	4	12	12	10	4	12	12	10	4	12	12	10	4
B10	IV	115	8	38	0.00	12	12	10	4	12	12	10	4	12	12	10	4	12	12	10	4
B11	IV	105	10	38	0.00	12	12	10	4	12	12	10	4	12	12	10	4	12	12	10	4
B12	IV	100	12	38	0.00	12	12	10	4	12	12	10	4	12	12	10	4	12	12	10	4
B13	IV	65	6	12	0.17	6	4	0	0	8	4	0	0	8	4	0	0	8	4	0	0
B14	IV	60	8	12	0.17	6	4	0	0	8	4	0	0	8	4	0	0	8	4	0	0
B15	IV	55	10	12	0.17	6	4	0	0	8	4	0	0	8	4	0	0	8	4	0	0
B16	IV	50	12	12	0.17	6	4	0	0	8	4	0	0	8	4	0	0	8	4	0	0
B17	IV	105	6	26	0.23	8	6	6	0	10	6	6	0	10	8	6	0	10	8	8	0
B18	IV	95	8	26	0.23	8	6	6	0	10	6	6	0	10	8	6	0	10	8	8	0
B19	IV	90	10	26	0.23	8	6	6	0	10	6	6	0	10	8	6	0	10	8	8	0
B20	IV	85	12	26	0.23	8	6	6	0	10	6	6	0	10	8	6	0	10	8	8	0
B21	IV	120	6	38	0.26	10	10	8	0	12	12	8	0	12	12	10	2	12	12	10	4
B22	IV	115	8	38	0.26	10	10	8	0	12	12	8	0	12	12	10	2	12	12	10	4
B23	IV	105	10	38	0.26	10	10	8	0	12	12	8	0	12	12	10	2	12	12	10	4
B24	IV	100	12	38	0.26	10	10	8	0	12	12	8	0	12	12	10	2	12	12	10	4

Table 8. (continued)

Case ID	AASHTO Type	Span Length	Spacing	Total strands	Max. debond ratio	Bonded Strands in each row (R) from the bottom of the girder															
						0' to 3'				3' to 6'				6' to 9'				9' to L/2			
		L (ft)	S (ft)	N	dr	R1	R2	R3	R4	R1	R2	R3	R4	R1	R2	R3	R4	R1	R2	R3	R4
B25	IV	65	6	12	0.50	4	2	0	0	6	2	0	0	8	2	0	0	8	4	0	0
B26	IV	60	8	12	0.50	4	2	0	0	6	2	0	0	8	2	0	0	8	4	0	0
B27	IV	55	10	12	0.50	4	2	0	0	6	2	0	0	8	2	0	0	8	4	0	0
B28	IV	50	12	12	0.50	4	2	0	0	6	2	0	0	8	2	0	0	8	4	0	0
B29	IV	105	6	26	0.46	6	4	4	0	8	6	4	0	10	8	4	0	10	8	8	0
B30	IV	95	8	26	0.46	6	4	4	0	8	6	4	0	10	8	4	0	10	8	8	0
B31	IV	90	10	26	0.46	6	4	4	0	8	6	4	0	10	8	4	0	10	8	8	0
B32	IV	85	12	26	0.46	6	4	4	0	8	6	4	0	10	8	4	0	10	8	8	0
B33	IV	120	6	38	0.47	8	8	4	0	10	10	8	0	12	12	8	2	12	12	10	4
B34	IV	115	8	38	0.47	8	8	4	0	10	10	8	0	12	12	8	2	12	12	10	4
B35	IV	105	10	38	0.47	8	8	4	0	10	10	8	0	12	12	8	2	12	12	10	4
B36	IV	100	12	38	0.47	8	8	4	0	10	10	8	0	12	12	8	2	12	12	10	4
B37	IV	65	6	12	0.67	2	2	0	0	4	4	0	0	6	4	0	0	8	4	0	0
B38	IV	60	8	12	0.67	2	2	0	0	4	4	0	0	6	4	0	0	8	4	0	0
B39	IV	55	10	12	0.67	2	2	0	0	4	4	0	0	6	4	0	0	8	4	0	0
B40	IV	50	12	12	0.67	2	2	0	0	4	4	0	0	6	4	0	0	8	4	0	0
B41	IV	105	6	26	0.77	4	2	0	0	8	4	2	0	10	6	4	0	10	8	8	0
B42	IV	95	8	26	0.77	4	2	0	0	8	4	2	0	10	6	4	0	10	8	8	0
B43	IV	90	10	26	0.77	4	2	0	0	8	4	2	0	10	6	4	0	10	8	8	0
B44	IV	85	12	26	0.77	4	2	0	0	8	4	2	0	10	6	4	0	10	8	8	0
B45	IV	120	6	38	0.74	4	4	2	0	10	8	4	0	12	10	6	2	12	12	10	4
B46	IV	115	8	38	0.74	4	4	2	0	10	8	4	0	12	10	6	2	12	12	10	4
B47	IV	105	10	38	0.74	4	4	2	0	10	8	4	0	12	10	6	2	12	12	10	4
B48	IV	100	12	38	0.74	4	4	2	0	10	8	4	0	12	10	6	2	12	12	10	4

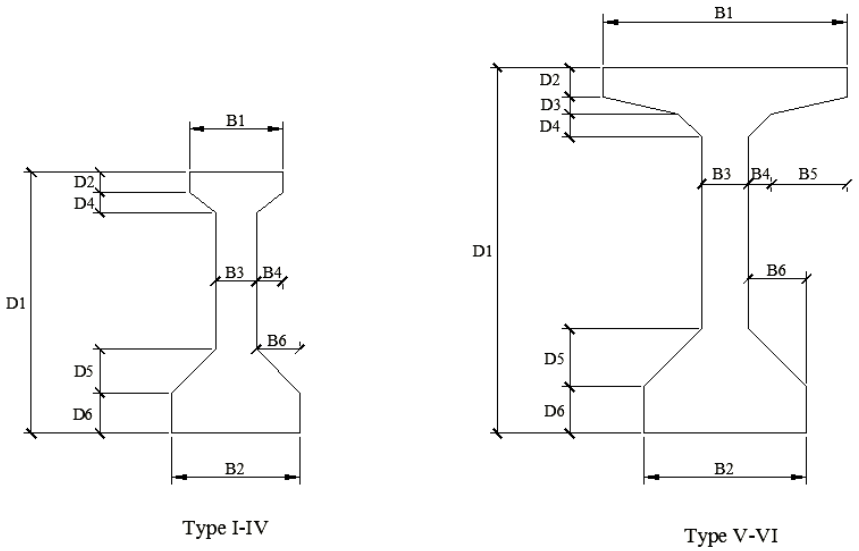

Figure 5. Section dimensions of AASHTO type girders
(adapted from Appendix-B of PCI Bridge Design Manual, 2011)

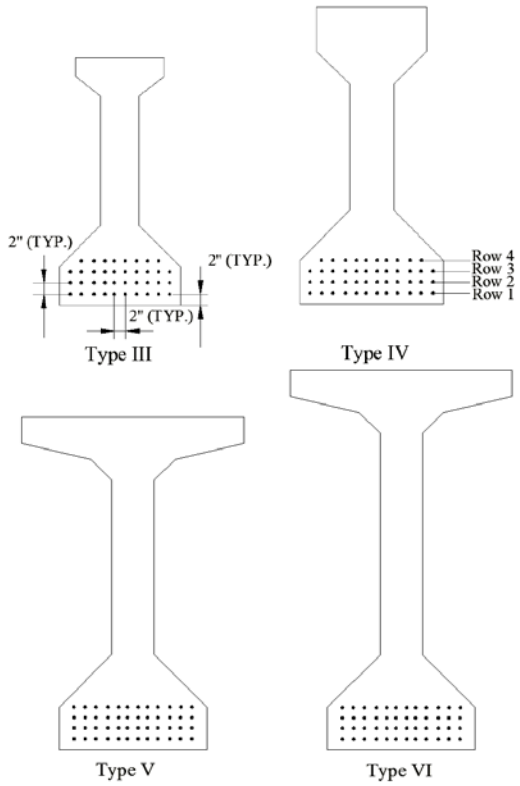

Figure 6. Strands arrangements of AASHTO I-girders
(adapted from Appendix-B of PCI Bridge Design Manual, 2011)

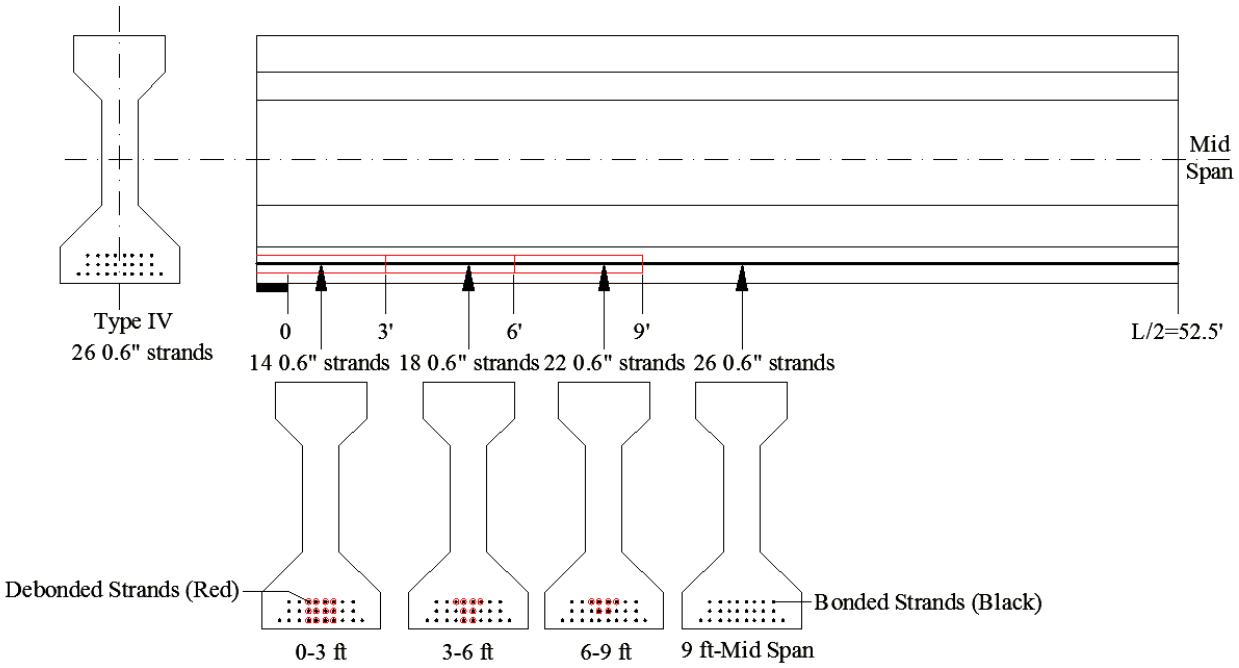

Figure 7. Example of partial debonding (Case B29 in Table 3-7)

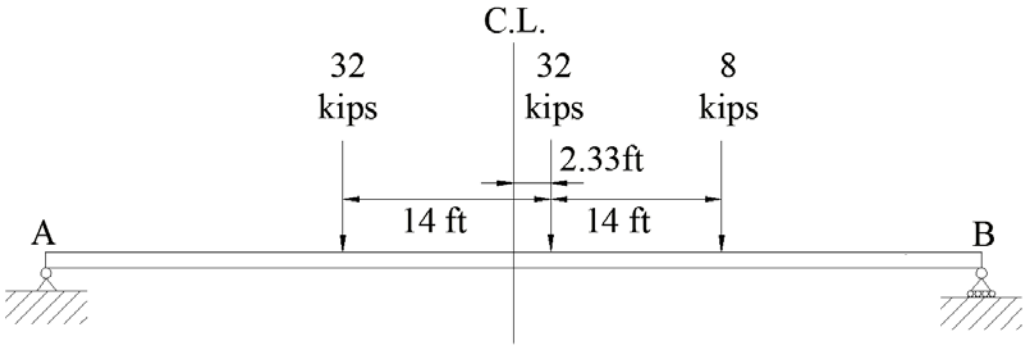

a) Location of HL-93 vehicle to cause maximum moment in span

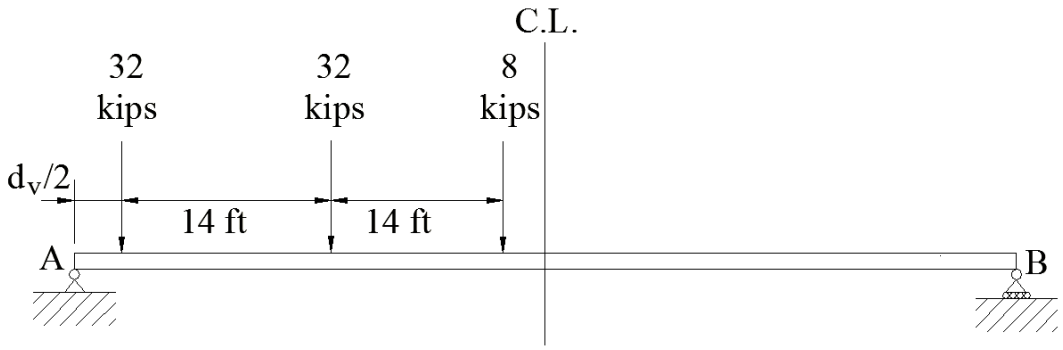

b) Location of HL-93 vehicle to cause maximum shear at shear critical section

Figure 8. Locations of design truck load at maximum moment and shear critical section

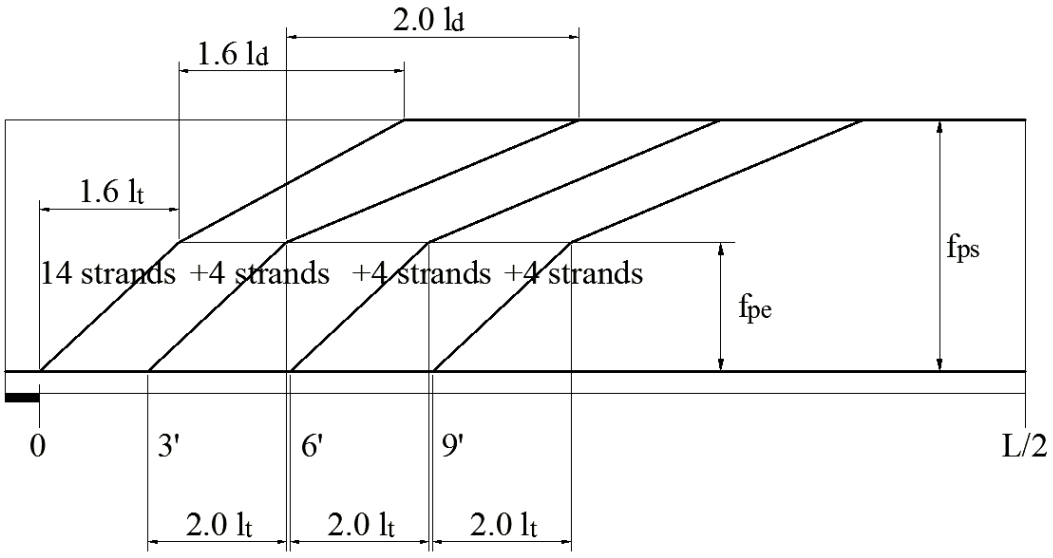

Figure 9. Schematic representation of development length (Case B29 in Table 3-7)

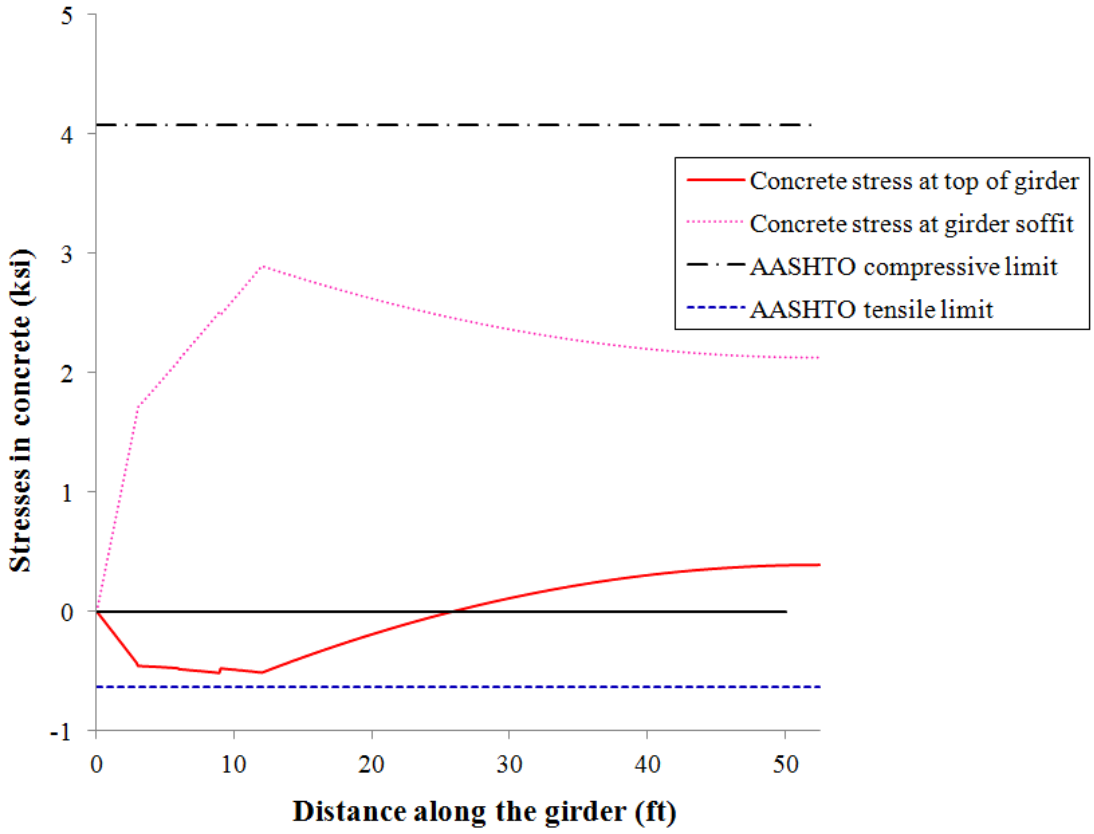

Figure 10. Compressive (positive) and tensile (negative) stress at prestress transfer

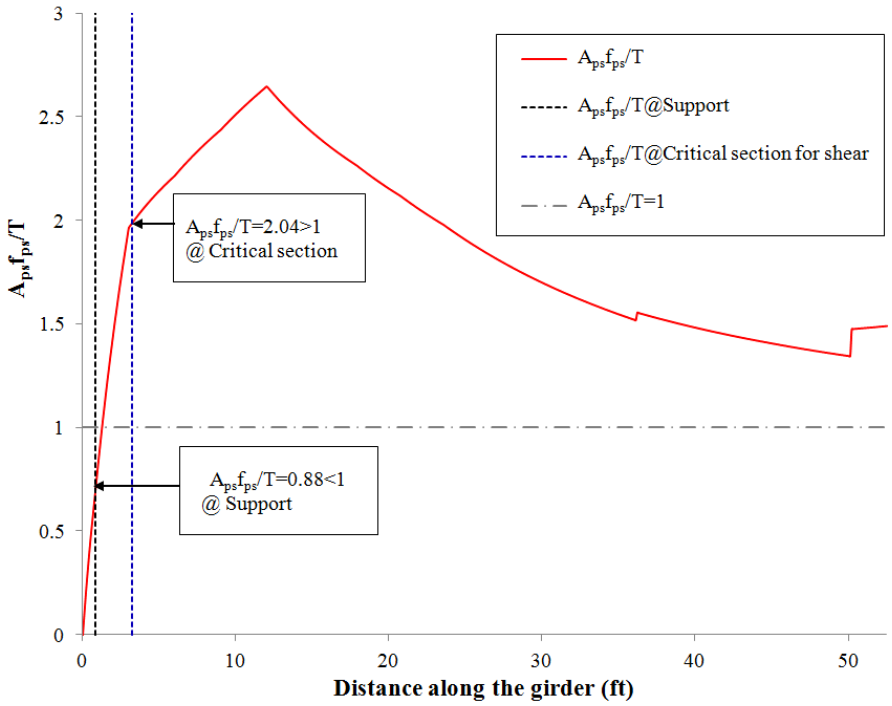

a) Capacity ratio of prestressing strands along the girder length

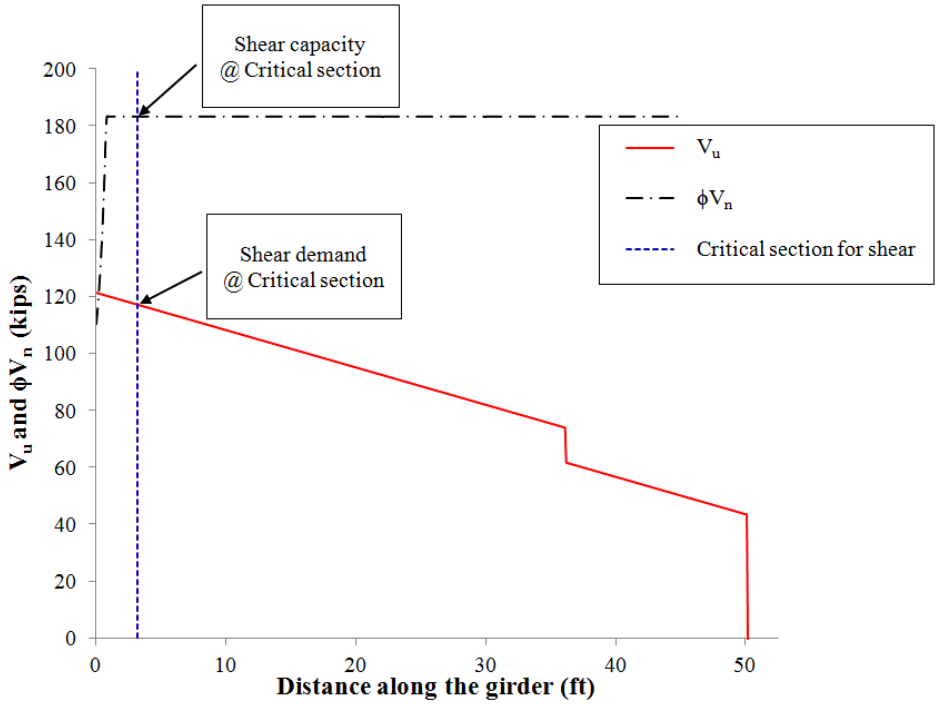

b) Shear capacity and demand along the girder length

Figure 11. Representative results from MATLAB analyses for Case B29 subjected to STENGTH I load combination with the HL-93 vehicle arranged for flexure (Figure 3-4a)

4.0 DISCUSSION OF RESULTS

4.1 VALIDATION OF MATLAB MODEL

Initial design capacities reported in the *PCI Bridge Design Manual* (2011) are adopted to validate the MATLAB-generated results, which strictly follow the AASHTO design procedures. The factored moment demand (M_u) and factored flexural resistance (ϕM_n) based on the MATLAB code and obtained from the PCI *Manual*, are listed in Tables 4-1 and 4-2, for Series A and B, respectively. Table 4-3 shows the average, minimum and maximum values for the comparison of M_u and ϕM_n, based on MATLAB code and PCI. Tables 4-1 and 4-2 also summarise the concrete tensile ($0.24\sqrt{f'_{ci}}/f_c$) and longitudinal tension ($A_{ps}f_{ps}/T$) capacity ratios obtained from the MATLAB analyses.

As seen in Tables 4-1 to 4-3, the MATLAB analysis yields a girder capacity slightly smaller and an applied moment slightly greater than those provided by PCI. Since the girder sections are generally 'well designed', it is expected that the results from MATLAB and PCI are in good agreement, neither over- or under-designed for the parameters considered. The reason for the reduced $\phi M_n/M_u$ margin in the MATLAB analyses may be attributed to the inclusion of the wearing surface load, DW (Section 3.2.4.2), which is not included in the PCI preliminary design calculations. Based on the results shown, it is verified that the MATLAB analyses represent the girder design behaviour quite well.

4.2 SERIES A

The concrete tensile stress ($0.24\sqrt{f'_{ci}}/f_{ct}$) and longitudinal tension capacity ($A_{ps}f_{ps}/T$) ratios for Series A (Table 4-1), in which the span length and total number of strands is held constant and the girder types are varying, are plotted as solid and dashed lines respectively, in Figure 4-1. In this figure, the total number of strands (12, 16, 28 and 40 strands) – and therefore the appropriate span lengths (50, 70, 100 and 125 ft) – increase from left to right on the horizontal axis. All four girder sizes, Type III through VI, are shown. Successful partial debonding must be sufficient to result in $0.24\sqrt{f'_{ci}}/f_{ct} \geq 1.0$ while maintaining enough bonded steel to ensure that $A_{ps}f_{ps}/T \geq 1.0$. Observations drawn from the results of the MATLAB analysis are as follows:

(1) Critical concrete tensile stress f_{ct} falls as the girder depth H increases (from girder type III to girder type VI). This observation reflects the fact that f_{ct} is a function of the inverse of section area (1/A) and section modulus ($1/S_t$) (Eqs 2-3 and 2-4). As the girder depth (H) increases, section area (A) increases essentially linearly, while section modulus (S_t) increases as H^2, thus f_{ct} decreases.

(2) The additional tensile force in the longitudinal reinforcement (T) (Eq. 2-9) will increase as girder depth H increases (from girder type III to VI). This is because, for a fixed number of strands, the factored moment (ϕM_u) and shear capacities (ϕV_u) increase with an increase of the girder depth H, thus T is increases.

(3) For shallower girders (Type III) having shorter spans, the $A_{ps}f_{ps}/T \geq 1\ 0$ is not satisfied at 0% debonding (consider Type III girders in Figure 4-1a). Thus, any debonding will make these critical girders more severe in terms of requiring mild steel to supplement the longitudinal tension capacity (A_s in Eq. 2-11). This is somewhat expected since the transfer and

development lengths are proportionally longer in relation to the girder depth and thus encroach further into the span where tension demands, T, are higher. Additionally for short shallow girders, in order to satisfy the $0.24\sqrt{f_{ci}}/f_{ct} \geq 1.0$ concrete tensile requirement, some degree of debonding is required (Figure 4-1a). Thus, short shallow spans are particularly critical and may: a) require supplemental mild steel to satisfy $A_{ps}f_{ps}/T \geq 1.0$; and/or b) require measures other than debonding (such as harping) to satisfy $0.24\sqrt{f_{ci}}/f_{ct} \geq 1.0$.

(4) For deeper girders (Type IV and larger) having longer spans and more prestressing strands, debonding is required to satisfy $0.24\sqrt{f_{ci}}/f_{ct} \geq 1.0$, although there is reserve capacity in the $A_{ps}f_{ps}/T \geq 1.0$ criteria to permit this. This can be seen in the case of 25% debonding shown in Figure 4-1b in which this degree of partial debonding reduces the concrete tensile stress in the beam, increasing $0.24\sqrt{f_{ci}}/f_{ct}$. Although partial debonding does reduce $A_{ps}f_{ps}$, the ratio $A_{ps}f_{ps}/T$ remains above unity for many cases, particularly those with a larger number of strands (Figure 4-1b). Greater debonding (Figures 4.1c and d) reduces the concrete tensile strengths but also reduce the area of prestressing strand A_{ps} to the extent that the $A_{ps}f_{ps}/T \geq 1.0$ criteria is no longer satisfied.

4.3 SERIES B

Maintaining the same girder section (Type IV), while the total number of strand and girder length are varying, the concrete tensile stress ($0.24\sqrt{f_{ci}}/f_{ct}$) and longitudinal tension capacity ($A_{ps}f_{ps}/T$) ratios (Table 4-2) for Series B plotted in Figure 4-2. Observations drawn from results of the MATLAB analysis are as follows:

(1) As total number of strand (N) increases, the concrete tensile stress ratio ($0.24\sqrt{f'_{ci}}/f_{ct}$) becomes more critical. For instance, this ratio is greater than unity for N=12, regardless of debonding ratio. However, this ratio is reduced greatly and is smaller than unity for both N=26 and N=38, regardless of the debonding ratio (the case of N = 26 with dr = 77% does, in fact, barely satisfy the $0.24\sqrt{f'_{ci}}/f_{ct}$ criteria). This is mainly because the strands are distributed at the bottom of the section, resulting in greater eccentric moment (Pe in Eq. 2-4) and therefore increasing f_{ct}. The longer span, (L) which results in more self-weight-induced moment, can mitigate this effect to some extent.

(2) With the same total strand number, $f_{ps}A_{ps}/T \geq 1.0$ is more critical for shorter spans than for longer spans. This is because for the shorter span, the factored shear force (V_u) is greater than for longer spans having the same moment capacity; this leads to a larger value of T (Eq. 2-9). For the same span length, $f_{ps}A_{ps}/T \geq 1.0$ is more critical at larger debonding ratios since $f_{ps}A_{ps}$ is smaller in this instance.

(3) Short beams having fewer strands easily satisfy the $0.24\sqrt{f'_{ci}}/f_{ct} \geq 1.0$ criteria. Since debonding will generally not be required for such shorter beams, additional mild steel may be needed to meet the $f_{ps}A_{ps}/T \geq 1.0$ criteria. In the cases shown in Figure 4-2, a Type IV girder having only 12 strands requires no debonding to satisfy concrete tension requirements but requires additional mild steel to meet the $f_{ps}A_{ps}/T \geq 1.0$ criteria for lengths less than about 62 ft.

(4) Longer beams having a large number of strands do not easily meet the $0.24\sqrt{f'_{ci}}/f_{ct} \geq 1.0$ criteria, despite being able to accommodate relatively large amounts of debonding. Thus harping will likely be required in addition to debonding to meet the concrete tension stress criteria. Longer beams can accommodate greater debonding but the debonding itself has a proportionally smaller impact on the concrete tension stresses.

4.4 ACCEPTABLE PARTIAL DEBONDING

This study aimed at establishing a reasonable range for the maximum partial debonding ratio permitted for AASHTO type girders. The successful debonding ratio must be sufficient to satisfy both the concrete tensile stress ratio: $0.24\sqrt{f'_{ci}}/f_{ct} \geq 1.0$ and the longitudinal tension capacity ratio: $A_{ps}f_{ps}/T \geq 1.0$.

To illustrate this requirement, an AASHTO type IV girder having a span of 105 ft and a total of 26 strands is selected as the example. Different debonding ratios – 0%, 23%, 46% and 77%, representing cases B5, B17, B29, and B41 in Table 4-2 are considered. The resulting capacity ratios are plotted against the debonding ratio in Figure 4-3. The location at which the trend line of $0.24\sqrt{f'_{ci}}/f_{ct}$ passes unity represents the minimum debonding ratio required to satisfy concrete tensile limits. The intersection of the $A_{ps}f_{ps}/T$ trend line with unity represents the maximum debonding ratio permitted that will still satisfy longitudinal steel stress requirement. In the case shown in Figure 4-3, the debonding ratio must exceed 0.31 to satisfy the concrete stress limit but may not exceed 0.39 in order to continue to satisfy the longitudinal tension requirement without the addition of mild steel; thus an acceptable debonding ratio falls between these values in this case. The acceptable range of debonding ratios varies with girder type, length, spacing, total number of strands and etc. Acceptable debonding ratios are summarized in Table 4-4 from which the following conclusions are drawn:

(1) The "unsuccessful" debonding ratios (N/A in the Table 4-4) primarily result because strand capacity ratio ($A_{ps}f_{ps}/T$) is difficult to achieve. Therefore other approaches, such as the addition of mild steel, should be implemented to improve the shear capacity of the girders.

(2) Acceptable debonding ratios may not be found for shorter spans (also having smaller number of strands). For example, both concrete and longitudinal steel criteria cannot be met for

50 ft and 70 ft AASHTO Type III girders, 50 to 65 ft AASHTO Type IV girders, and 70 ft AASHTO Type V and VI girders. This means, in most cases, that even fully bonded strands cannot meet the strand capacity requirement ($A_{ps}f_{ps}/T>1.0$). Additional mild steel is therefore required in the end regions for shorter span girders.

(3) With an increase of girder height (from Type III to Type IV), it is more likely to obtain acceptable debonding ratios due to the greater efficiency of the remaining bonded strands over a longer lever arm (d_v in Eq. 2-10).

(4) The acceptable range of debonding ratios is relatively small for moderate span lengths and becomes broader for longer spans. Consider the example of Type V girders:, the acceptable range of debonding ratio for 100 ft (with 28 total strands) is 0.04-0.10; this increases to 0.35-0.45 for L = 125 ft (with 40 total strands).

While the range of acceptable debonding ratio may seem restricted, it must be recalled that the ranges provided are based on both concrete and longitudinal tension criteria. The 'upper' limit on the range is a function of the $A_{ps}f_{ps}/T$ criteria. The only way to increase this is to provide additional mild steel, a detail that is often considered impractical, particularly in heavily reinforced sections. The lower limit, on the other hand, is a function of the $0.24\sqrt{f'_{ci}}/f_{ct}$ criteria. This may be partially or even fully addressed by harping strands or by the addition of prestressed reinforcement at the top of the section (this is often sacrificial and is cut at some point in the erection process, usually following the application of the deck). Thus, were a limit is shown in Table 4-3, the range may be practically extended downward, but not upward.

Table 9. Results of Series A

Case ID	AASHTO Type	Span Length	Spacing	Total strands	Max. debond ratio	$\frac{0.24\sqrt{f_{ci}}}{f_c}$	$\frac{A_{ps}f_{ps}}{T}$		MATLAB values			PCI values			MATLAB PCI	
							support	critical section	ϕM_n	M_u	$\frac{\phi M_n}{Mu}$	ϕM_r	M_u	$\frac{\phi M_r}{M_u}$	M_n	M_u
		L (ft)	S (ft)	N	dr				(kip-ft)			(kip-ft)				
A1	III	70	8	16	0.00	0.70	0.97	1.99	3693	3847	0.96	3862	3669	1.05	0.96	1.05
A2	IV	70	10	16	0.00	0.98	0.88	1.87	4462	4883	0.91	4658	4586	1.02	0.96	1.06
A3	V	70	10	16	0.00	1.58	0.95	2.05	5162	5183	1.00	5322	4945	1.08	0.97	1.05
A4	VI	70	12	16	0.00	1.64	0.86	1.89	5920	6063	0.98	6127	5656	1.08	0.97	1.07
A5	III	100	6	28	0.00	0.44	1.60	3.37	5961	5519	1.08	6214	5402	1.15	0.96	1.02
A6	IV	100	8	28	0.00	0.60	1.41	3.06	7340	7309	1.00	7667	6940	1.10	0.96	1.05
A7	V	100	10	28	0.00	0.95	1.26	2.80	8728	9109	0.96	9000`	8623	1.04	0.97	1.06
A8	VI	100	12	28	0.00	0.98	1.13	2.58	10084	10663	0.95	10438	9864	1.06	0.97	1.08
A9	III	50	10	12	0.00	0.88	0.74	1.49	2882	2694	1.07	3003	2543	1.18	0.96	1.06
A10	IV	50	12	12	0.00	1.25	0.69	1.44	3435	3311	1.04	3622	3111	1.16	0.95	1.06
A11	V	50	12	12	0.00	2.02	0.75	1.58	3957	3491	1.13	-	-	-	-	-
A12	IV	125	6	40	0.00	0.44	2.08	4.38	9662	8723	1.11	9541	8532	1.12	1.01	1.02
A13	V	125	8	40	0.00	0.69	1.78	4.00	11794	11258	1.05	12287	11454	1.07	0.96	0.98
A14	VI	125	10	40	0.00	0.70	1.55	3.57	13970	13461	1.03	14242	13347	1.07	0.98	1.01
A15	III	70	8	16	0.25	0.95	0.73	1.56	3693	3847	0.96	3862	3669	1.05	0.96	1.05
A16	IV	70	10	16	0.25	1.36	0.66	1.46	4462	4883	0.91	4658	4586	1.02	0.96	1.06
A17	V	70	10	16	0.25	2.21	0.71	1.60	5162	5183	1.00	5322	4945	1.08	0.97	1.05
A18	VI	70	12	16	0.25	2.29	0.65	1.48	5920	6063	0.98	6127	5656	1.08	0.97	1.07
A19	III	100	6	28	0.21	0.56	1.25	2.70	5961	5519	1.08	6214	5402	1.15	0.96	1.02
A20	IV	100	8	28	0.21	0.78	1.11	2.46	7340	7309	1.00	7667	6940	1.10	0.96	1.05
A21	V	100	10	28	0.21	1.24	0.99	2.25	8728	9109	0.96	9000	8623	1.04	0.97	1.06
A22	VI	100	12	28	0.21	1.27	0.89	2.07	10084	10663	0.95	10438	9864	1.06	0.97	1.08
A23	III	50	10	12	0.17	1.00	0.63	1.31	2882	2694	1.07	3003	2543	1.18	0.96	1.06

Table 9. (continued)

Case ID	AASHTO Type	Span Length	Spacing	Total strands	Max. debond ratio	$\frac{0.24\sqrt{f_{ci}}}{f_c}$	$\frac{A_{ps}f_{ps}}{T}$		MATLAB values			PCI values			$\frac{\text{MATLAB}}{\text{PCI}}$	
							support	critical section	ϕM_n	M_u	$\frac{\phi M_n}{Mu}$	ϕM_r	M_u	$\frac{\phi M_r}{M_u}$	M_n	M_u
		L (ft)	S (ft)	N	dr				(kip-ft)			(kip-ft)				
A24	IV	50	12	12	0.17	1.44	0.60	1.26	3435	3311	1.04	3622	3111	1.16	0.95	1.06
A25	V	50	12	12	0.17	2.36	0.64	1.39	3957	3491	1.13	-	-	-	-	-
A26	IV	125	6	40	0.25	0.58	1.56	3.34	9662	8723	1.11	9541	8532	1.12	1.01	1.02
A27	V	125	8	40	0.25	0.91	1.34	3.10	11794	11258	1.05	12287	11454	1.07	0.96	0.98
A28	VI	125	10	40	0.25	0.94	1.16	2.77	13970	13461	1.03	14242	13347	1.07	0.98	1.01
A29	III	70	8	16	0.50	0.95	0.52	1.12	3693	3847	0.96	3862	3669	1.05	0.96	1.05
A30	IV	70	10	16	0.50	1.39	0.49	1.05	4462	4883	0.91	4658	4586	1.02	0.96	1.06
A31	V	70	10	16	0.50	2.34	0.52	1.15	5162	5183	1.00	5322	4945	1.08	0.97	1.05
A32	VI	70	12	16	0.50	2.33	0.48	1.07	5920	6063	0.98	6127	5656	1.08	0.97	1.07
A33	III	100	6	28	0.50	0.69	0.80	1.79	5961	5519	1.08	6214	5402	1.15	0.96	1.02
A34	IV	100	8	28	0.50	1.00	0.71	1.64	7340	7309	1.00	7667	6940	1.10	0.96	1.05
A35	V	100	10	28	0.50	1.67	0.63	1.50	8728	9109	0.96	9000	8623	1.04	0.97	1.06
A36	VI	100	12	28	0.50	1.59	0.58	1.38	10084	10663	0.95	10438	9864	1.06	0.97	1.08
A37	III	50	10	12	0.50	1.12	0.43	0.81	3437	3311	1.07	3003	2543	1.18	1.14	1.30
A38	IV	50	12	12	0.50	1.66	0.42	0.79	3437	3311	1.04	3622	3111	1.16	0.95	1.06
A39	V	50	12	12	0.50	2.77	0.44	0.86	3957	3491	1.13	-	-	-	-	-
A40	IV	125	6	40	0.50	0.71	1.04	2.53	9662	8723	1.11	9541	8532	1.12	1.01	1.02
A41	V	125	8	40	0.50	1.16	0.89	2.15	11794	11258	1.05	12287	11454	1.07	0.96	0.98
A42	VI	125	10	40	0.50	1.10	0.77	1.92	13970	13461	1.03	14242	13347	1.07	0.98	1.01
A43	III	70	8	16	0.75	1.11	0.33	0.66	3693	3847	0.96	3862	3669	1.05	0.96	1.05
A44	IV	70	10	16	0.75	1.70	0.33	0.63	4462	4883	0.91	4658	4586	1.02	0.96	1.06
A45	V	70	10	16	0.75	2.95	0.34	0.68	5162	5183	1.00	5322	4945	1.08	0.97	1.05
A46	VI	70	12	16	0.75	2.83	0.33	0.64	5920	6063	0.98	6127	5656	1.08	0.97	1.07
A47	III	100	6	28	0.71	0.69	0.48	1.13	5961	5519	1.08	6214	5402	1.15	0.96	1.02

Table 9. (continued)

Case ID	AASHTO Type	Span Length	Spacing	Total strands	Max. debond ratio	$\frac{0.24\sqrt{f_{ci}}}{f_c}$	$\frac{A_{ps}f_{ps}}{T}$		MATLAB values			PCI values			$\frac{\text{MATLAB}}{\text{PCI}}$	
							support	critical section	ϕM_n	M_u	$\frac{\phi M_n}{Mu}$	ϕM_r	M_u	$\frac{\phi M_r}{M_u}$	M_n	M_u
		L (ft)	S (ft)	N	dr				(kip-ft)			(kip-ft)				
A48	IV	100	8	28	0.71	1.00	0.45	1.04	7340	7309	1.00	7667	6940	1.10	0.96	1.05
A49	V	100	10	28	0.71	1.67	0.42	0.95	8728	9109	0.96	9000	8623	1.04	0.97	1.06
A50	VI	100	12	28	0.71	1.59	0.40	0.88	10084	10663	0.95	10438	9864	1.06	0.97	1.08
A51	III	50	10	12	0.67	1.26	0.34	0.66	3437	3311	1.07	3003	2543	1.18	1.14	1.30
A52	IV	50	12	12	0.67	1.89	0.33	0.65	3435	3311	1.04	3622	3111	1.16	0.95	1.06
A53	V	50	12	12	0.67	3.24	0.35	0.70	3957	3491	1.13	-	-	-	-	-
A54	IV	125	6	40	0.70	0.71	0.63	1.49	9662	8723	1.11	9541	8532	1.12	1.01	1.02
A55	V	125	8	40	0.70	1.16	0.55	1.45	11794	11258	1.05	12287	11454	1.07	0.96	0.98
A56	VI	125	10	40	0.70	1.10	0.50	1.29	13970	13461	1.03	14242	13347	1.07	0.98	1.01

Table 10. Results of Series B

Case ID	AASHTO Type	Span Length	Spacing	Total strands	Max. debond ratio	$\frac{0.24\sqrt{f_{ci}}}{f_c}$	$\frac{A_{ps}f_{ps}}{T}$		MATLAB values			PCI values			MATLAB / PCI	
							support	critical section	ϕM_n	M_n	M_u	support	critical section	ϕM_n	M_n	M_u
		L (ft)	S (ft)	N	dr				(kip-ft)			(kip-ft)				
B1	IV	65	6	12	0.00	1.31	1.13	2.29	3311	3077	1.08	3467	3014	1.15	0.95	1.02
B2	IV	60	8	12	0.00	1.29	0.90	1.86	3344	3289	1.02	3501	3146	1.11	0.96	1.05
B3	IV	55	10	12	0.00	1.27	0.78	1.61	3392	3361	1.01	3550	3171	1.12	0.96	1.06
B4	IV	50	12	12	0.00	1.25	0.69	1.44	3435	3311	1.04	3622	3111	1.16	0.95	1.06
B5	IV	105	6	26	0.00	0.66	1.65	3.54	6706	6566	1.02	7030	6423	1.09	0.95	1.02
B6	IV	95	8	26	0.00	0.65	1.37	2.95	6852	6736	1.02	7246	6933	1.05	0.95	0.97
B7	IV	90	10	26	0.00	0.64	1.17	2.54	7004	7238	0.97	7334	6760	1.08	0.95	1.07
B8	IV	85	12	26	0.00	0.64	1.04	2.26	7127	7574	0.94	7522	7064	1.06	0.95	1.07
B9	IV	120	6	38	0.00	0.46	2.06	4.49	9268	8157	1.14	9571	8422	1.14	0.97	0.97
B10	IV	115	8	38	0.00	0.46	1.66	3.64	9634	9149	1.05	10011	8672	1.15	0.96	1.06
B11	IV	105	10	38	0.00	0.45	1.46	3.21	9910	9253	1.07	10372	9093	1.14	0.96	1.02
B12	IV	100	12	38	0.00	0.45	1.29	2.86	10128	9809	1.03	10606	9126	1.16	0.95	1.07
B13	IV	65	6	12	0.17	1.62	0.94	2.01	3311	3077	1.08	3467	3014	1.15	0.95	1.02
B14	IV	60	8	12	0.17	1.56	0.75	1.63	3344	3289	1.02	3501	3146	1.11	0.96	1.05
B15	IV	55	10	12	0.17	1.49	0.66	1.41	3392	3361	1.01	3550	3171	1.12	0.96	1.06
B16	IV	50	12	12	0.17	1.44	0.60	1.26	3435	3311	1.04	3622	3111	1.16	0.95	1.06
B17	IV	105	6	26	0.23	0.88	1.27	2.79	6706	6566	1.02	7030	6423	1.09	0.95	1.02
B18	IV	95	8	26	0.23	0.86	1.05	2.33	6852	6736	1.02	7246	6933	1.05	0.95	0.97
B19	IV	90	10	26	0.23	0.85	0.90	2.00	7004	7238	0.97	7334	6760	1.08	0.95	1.07
B20	IV	85	12	26	0.23	0.84	0.80	1.78	7127	7574	0.94	7522	7064	1.06	0.95	1.07
B21	IV	120	6	38	0.26	0.61	1.52	3.42	9268	8157	1.14	9571	8422	1.14	0.97	0.97
B22	IV	115	8	38	0.26	0.60	1.22	2.77	9634	9149	1.05	10011	8672	1.15	0.96	1.06
B23	IV	105	10	38	0.26	0.59	1.07	2.45	9910	9253	1.07	10372	9093	1.14	0.96	1.02
B24	IV	100	12	38	0.26	0.58	0.95	2.18	10128	9809	1.03	10606	9126	1.16	0.95	1.07

Table 10. (continued)

Case ID	AASHTO Type	Span Length	Spacing	Total strands	Max. debond ratio	$\frac{0.24\sqrt{f_{ci}}}{f_c}$	$\frac{A_{ps}f_{ps}}{T}$		MATLAB values			PCI values			MATLAB PCI	
							support	critical section	ϕM_n	M_n	M_u	support	critical section	ϕM_n	M_n	M_u
		L (ft)	S (ft)	N	dr				(kip-ft)			(kip-ft)				
B25	IV	65	6	12	0.50	2.70	0.59	1.24	3311	3077	1.08	3467	3014	1.15	0.95	1.02
B26	IV	60	8	12	0.50	2.36	0.50	1.01	3344	3289	1.02	3501	3146	1.11	0.96	1.05
B27	IV	55	10	12	0.50	2.10	0.45	0.87	3392	3361	1.01	3550	3171	1.12	0.96	1.06
B28	IV	50	12	12	0.50	1.89	0.42	0.79	3435	3311	1.04	3622	3111	1.16	0.95	1.06
B29	IV	105	6	26	0.46	1.22	0.89	2.04	6706	6566	1.02	7030	6423	1.09	0.95	1.02
B30	IV	95	8	26	0.46	1.09	0.74	1.70	6852	6736	1.02	7246	6933	1.05	0.95	0.97
B31	IV	90	10	26	0.46	1.03	0.63	1.47	7004	7238	0.97	7334	6760	1.08	0.95	1.07
B32	IV	85	12	26	0.46	0.98	0.57	1.31	7127	7574	0.94	7522	7064	1.06	0.95	1.07
B33	IV	120	6	38	0.47	0.70	1.08	2.60	9268	8157	1.14	9571	8422	1.14	0.97	0.97
B34	IV	115	8	38	0.47	0.69	0.87	2.10	9634	9149	1.05	10011	8672	1.15	0.96	1.06
B35	IV	105	10	38	0.47	0.65	0.77	1.86	9910	9253	1.07	10372	9093	1.14	0.96	1.02
B36	IV	100	12	38	0.47	0.63	0.68	1.65	10128	9809	1.03	10606	9126	1.16	0.95	1.07
B37	IV	65	6	12	0.67	2.70	0.44	0.96	3311	3077	1.08	3467	3014	1.15	0.95	1.02
B38	IV	60	8	12	0.67	2.36	0.38	0.79	3344	3289	1.02	3501	3146	1.11	0.96	1.05
B39	IV	55	10	12	0.67	2.10	0.35	0.70	3392	3361	1.01	3550	3171	1.12	0.96	1.06
B40	IV	50	12	12	0.67	1.89	0.33	0.65	3435	3311	1.04	3622	3111	1.16	0.95	1.06
B41	IV	105	6	26	0.77	1.23	0.44	1.09	6706	6566	1.02	7030	6423	1.09	0.95	1.02
B42	IV	95	8	26	0.77	1.09	0.39	0.91	6852	6736	1.02	7246	6933	1.05	0.95	0.97
B43	IV	90	10	26	0.77	1.03	0.35	0.78	7004	7238	0.97	7334	6760	1.08	0.95	1.07
B44	IV	85	12	26	0.77	0.70	0.33	0.18	7127	7574	0.94	7522	7064	1.06	0.95	1.07
B45	IV	120	6	38	0.74	0.74	0.55	1.54	9268	8157	1.14	9571	8422	1.14	0.97	0.97
B46	IV	115	8	38	0.74	0.71	0.47	1.23	9634	9149	1.05	10011	8672	1.15	0.96	1.06
B47	IV	105	10	38	0.74	0.66	0.43	1.10	9910	9253	1.07	10372	9093	1.14	0.96	1.02
B48	IV	100	12	38	0.74	0.64	0.39	0.98	10128	9809	1.03	10606	9126	1.16	0.95	1.07

Table 11. Validation of MATLAB analyses

	Average Value	COV	minimum	maximum
M_n MATLAB/M_n PCI	0.96	3.1%	0.95	1.14
M_u MATLAB/M_u PCI	1.05	4.7%	0.97	1.30
$\varphi M_n/M_u$ (in MATLAB)	1.02	5.6%	0.91	1.14
$\varphi M_n/M_u$ (in PCI)	1.10	4.1%	1.02	1.18

Table 12. Acceptable partial debonding ratio for AASHTO type girders

AASHTO Type	Series	Span Length (ft)	Total no. of strands	acceptable debonding ratio	Comments
III	A	50	12	N/A	$A_{ps}f_{ps}/T<1.0$
		70	16	N/A	$A_{ps}f_{ps}/T<1.0$
IV	A	70	16	N/A	$A_{ps}f_{ps}/T<1.0$
		100	28	0.45-0.55	
		125	40	0.65	
	B	50-65	12	N/A	$A_{ps}f_{ps}/T<1.0$
		85-105	26	0.20-0.50	
		100-120	36	0.75	
V	A	70	16	N/A	$A_{ps}f_{ps}/T<1.0$
		100	28	0.04-0.10	
		125	40	0.35-0.45	
VI	A	70	16	N/A	$A_{ps}f_{ps}/T<1.0$
		100	28	0.07-0.12	
		125	40	0.34-0.37	

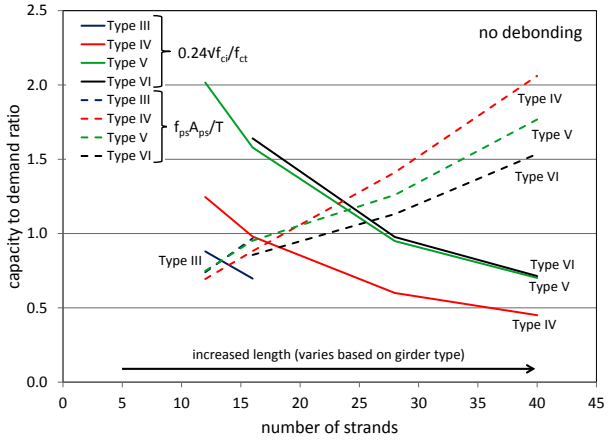

(a) no debonding

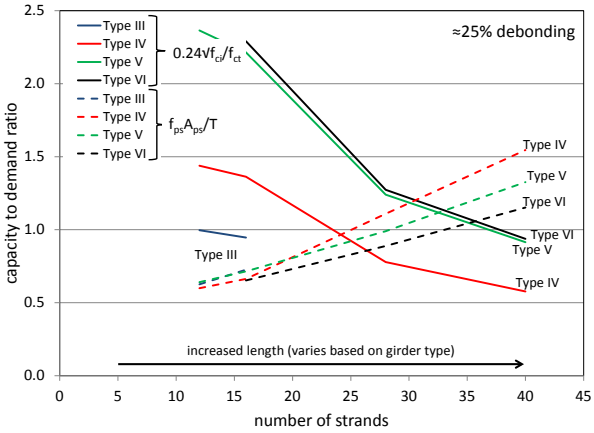

(b) approximately 25% debonding

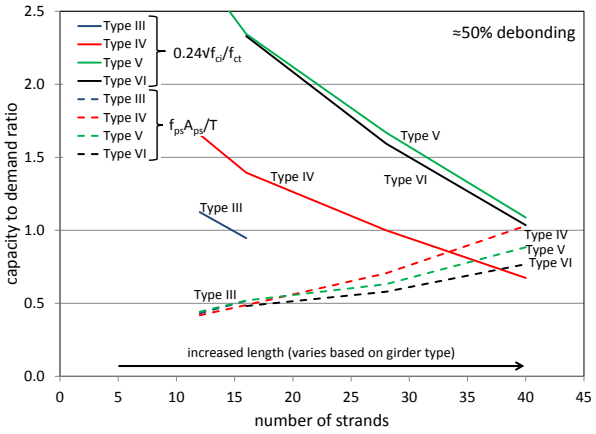

(c) 50% debonding

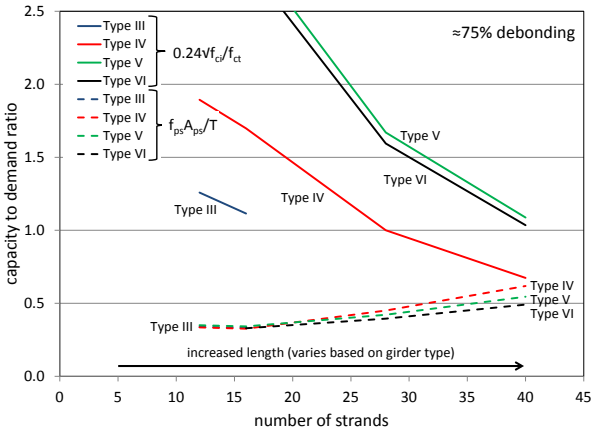

(d) approximately 75% debonding

Figure 12. Concrete tension and prestressing steel tension capacity ratios for AASHTO shapes having the same number of strands (N)

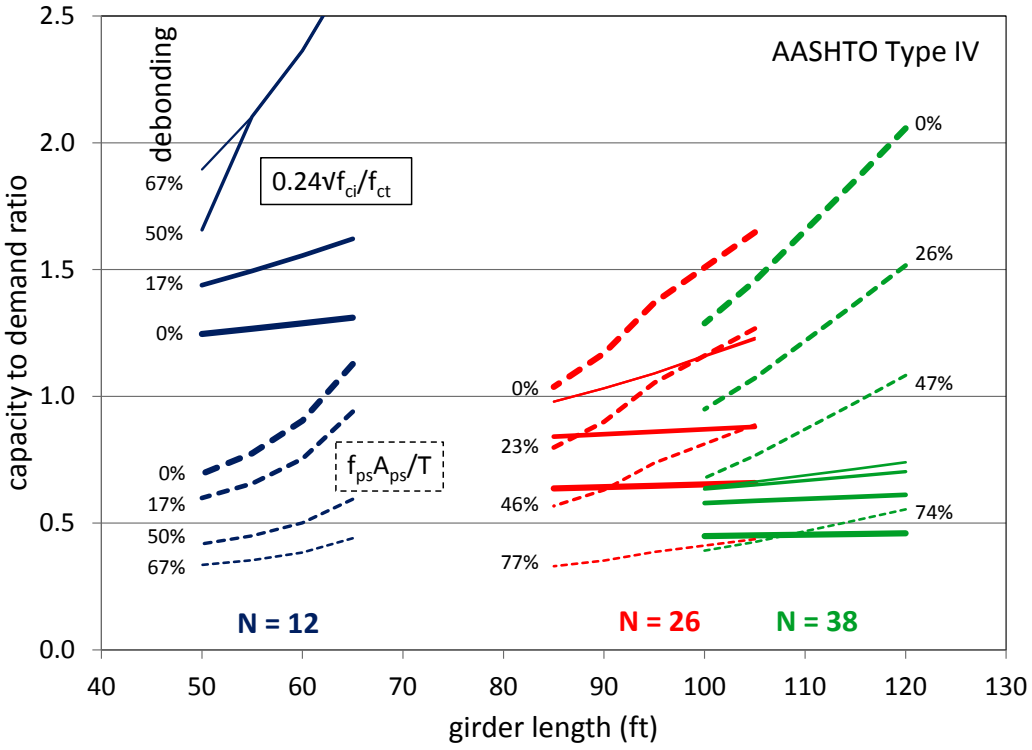

Figure 13. Concrete tension and prestressing steel tension capacity ratios for AASHTO Type IV girders shapes having varying lengths and strand arrangements

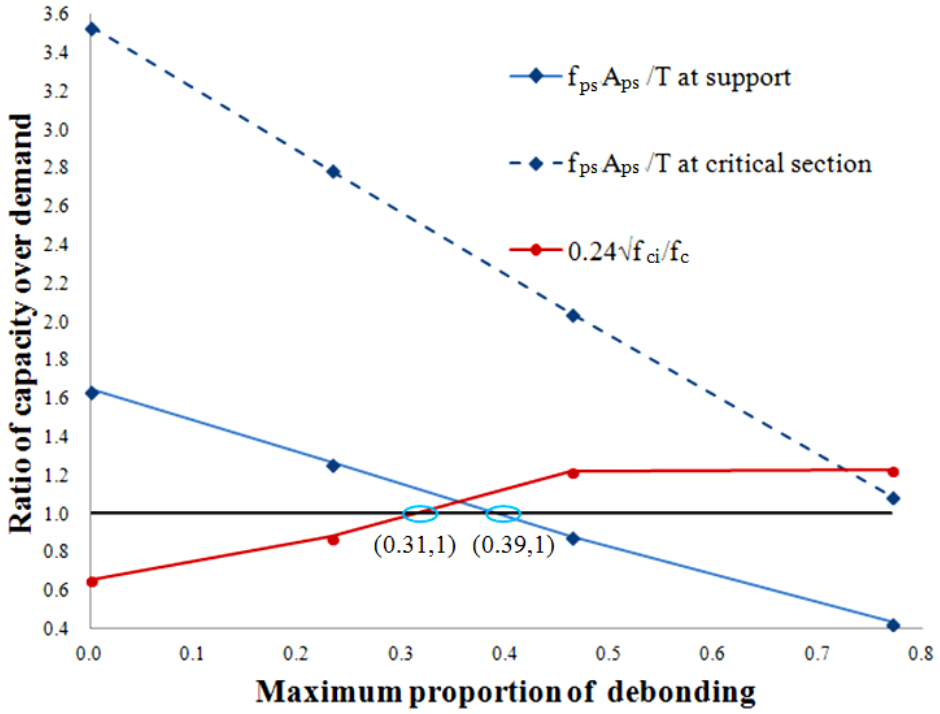

Figure 14. Representative example of capacity ratios (cases B5, B17, B29, and B41 shown)

5.0 CONCLUSIONS AND FUTURE WORKS

An overview of the conclusions and findings from this work are presented. Additionally, topics identified which require further investigation are also introduced.

5.1 CONCLUSIONS

In prestressed concrete girders, the strands are initially stressed, the concrete is placed, and once concrete strength has achieved a minimum specified value the prestress force is transferred to the concrete. At prestress transfer eccentrically located strands introduce flexure into prestressed concrete girders. This flexure typically results in upward camber of the girder, which will eventually be overcome by the application of structural loads. Camber results in tension at the top face of the member and compression at the bottom (Eq. 2-3); these stresses are only mitigated by the self-weight of the member at release (Eq. 2-4).

Near the girder ends, the effect of self-weight is negligible and the tensile stress often exceeds the cracking stress of the concrete – particularly since the concrete is typically several days old at the time of prestress transfer. The potential cracking is not only a structural concern but affects durability, especially in bridge structures where the top surface of girders may eventually be subject to wetting or water ingress. For this reason, the AASHTO *Specifications* (2010) limit the allowable tensile stress at prestress transfer to $0.0948\sqrt{f_{ci}}$; where f_{ci} = the

concrete compressive stress at prestress transfer measured in the unit of ksi. This is hard to meet and may be increased to $0.24\sqrt{f'_{ci}}$, where mild reinforcement for controlling cracking is provided. Nonetheless, with long girders requiring large amounts of prestressing strands, even the latter is difficult to meet.

There are two primary means of reducing the tensile stress at girder ends: a) harping strands to reduce the eccentricity and therefore the applied moment due to prestress force and b) debonding strands, resulting in reduced prestress force near the girder ends. Debonding was the focus of the present work. Debonding involves 'blanketing' the strands near their ends so that they may not bond to the concrete. Once the mitigating effect of girder self-weight is large enough to overcome the effect of camber and maintain the value of $f_c \leq 0.24\sqrt{f_{ci}}$, the blanketing is terminated and bond is allowed to develop. In this case the transfer and development lengths of the blanketed strands does not initiate at the girder end but at the termination of the blanketing. This process is referred to as 'partial debonding'. The ratio of debonded strands to the total number of strands in the girder is referred to as the debonding ratio and is the parameter of girder design that is the focus of this work

Two series of 26 AASHTO Type III-VI girders with different debonding ratios are analyzed using a MATLAB-based procedure. All analysis is based on and consistent with AASHTO *LRFD Specification* requirements. The results from AASHTO are validated by comparing these with the initial design values given in the *PCI Bridge Design Manual* (2011). To illustrate the analysis procedure, an individual case (Case B29, representing a 105 foot long Type IV girder having 26 0.6 in. strands) is presented in detail. The objective of the extensive parametric study presented is to establish an acceptable range or limits for debonding ratio.

The criteria for establishing an acceptable debonding ratio assumes that the girder will not failure under the external loads (i.e.: $\varphi M_n/M_u \geq 1.0$) and that the concrete tension stress limit at prestress transfer and the longitudinal tension capacity of the prestressing strand provided are both satisfied. That is: $0.24\sqrt{f'_{ci}}/f_{ct} \geq 1.0$ and $A_{ps}f_{ps}/T \geq 1.0$, respectively. The following conclusions are drawn:

1. The inability to establish a "successful" debonding ratio satisfying both criteria primarily results because strand capacity ratio ($A_{ps}f_{ps}/T$) is difficult to achieve. Therefore other approaches, such as the addition of mild steel, should be implemented to improve the shear capacity of the girders (Eqs 2.11 and 2.12). This is especially the case for shallower girders with shorter spans.
2. For girders having the same number of strands (N), $f_{ps}A_{ps}/T \geq 1.0$ is more critical for shorter spans than for longer spans.
3. As the total number of strand (N) increases, the concrete tensile stress ratio ($0.24\sqrt{f'_{ci}}/f_{ct}$) becomes more and more critical. Longer beams having a large number of strands do not easily meet this criteria.
4. With an increase of girder depth (from Type III to Type IV), it is more likely to obtain acceptable debonding ratios due to the greater efficiency of the remaining bonded strands over a longer lever arm (d_v in Eq. 2-10).
5. The acceptable range of debonding ratios is relatively small for moderate span lengths and becomes broader for longer spans.

Although the range of acceptable debonding ratio may seem restricted (Table 4-4), it must be noted that the ranges provided are based on both concrete and longitudinal tension criteria. The 'upper' limit on the range is a function of the $A_{ps}f_{ps}/T \geq 1.0$ criteria. The only way to increase

this is to provide additional mild steel, a detail that is often considered impractical, particularly in heavily reinforced sections. The lower limit, on the other hand, is a function of the $0.24\sqrt{f'_{ci}}/f_{ct} \geq 1.0$ criteria. This may be partially or even fully addressed by harping strands or by the addition of prestressed reinforcement at the top of the section.

Considering the results obtained for AASHTO Type girders, it appears that the upper limit for an acceptable debonding ratio may be increased from the current AASHTO-prescribed 25% to perhaps 50%. However the results also indicate that this upper limit is a function of span length, where the limit may be greater for longer spans, particularly given that no amount of debonding was found to be acceptable for shorter spans. Considerable further parametric study is required to establish such a relationship and to extend this work to other girder shapes.

5.2 TOPICS FOR TUTURE INVESTIGATION

5.2.1 Transfer and Development Lengths

In this study, the MATLAB program based on 2-D model and AASHTO *LRFD Specification* can accurately capture the mechanical behaviour of the span (B-region of the beam where the behavior follows that of a Bernoulli beam). However, near the span ends (D-region or 'disturbed' region), where the strands are developed and debonded, more study is needed.

Firstly, AASHTO *LRFD Specification* gives relatively conservative transfer and development length values and makes the assumption of uniform bond stress; these assumptions may be conservative for B-region design but are not necessarily so near the span ends. Shorter 'real-world' transfer lengths may increase concrete tension and therefore lead to a greater need

for debonding. However, those same short lengths improve the $A_{ps}f_{ps}/T$ since f_{ps} is greater for a shorter development length. Experimental study which can accurately predict the real transfer and development lengths are needed.

Secondly, the MATLAB program approach (essentially a plane-sections analysis) is inaccurate when predicting mechanical behaviour of the end D-regions. Three-dimensional finite element simulations which consider the "Hoyer effect" and transverse load spreading associated with strand patters are required. Adopting a representative bond-slip model and a reasonable concrete damage model are crucial to simulating the end region behavior.

5.2.2 Crack Distribution

Cracks occurring along the transfer length dimension are detrimental since they may lead to corrosion and ultimately failure of bond. The cracking that may occur in a typically end region are schematically shown in Figure 5-1. These cracks, even with small width, will gradually create a path for the ingress of corrosive substances and therefore, may lead to deterioration of the bond between the steel strands and surrounding concrete. Such deterioration may significantly impact the $A_{ps}f_{ps}/T$ criteria by reducing both f_{ps} (reduced bond) and A_{ps} (loss of section due to corrosion). Although distributing the partial debonding along the pretensioned beam can effectively reduce the stress concentration at the end region and thus mitigate longitudinal splitting and some web cracking, new cracks may also occur at the terminations of the debonding due to stress concentrations at these locations. How to predict the crack width for both fully bonded and partially bonded pretensioned girders, as well as evaluating the corrosion resulted from cracks, should be carefully studied.

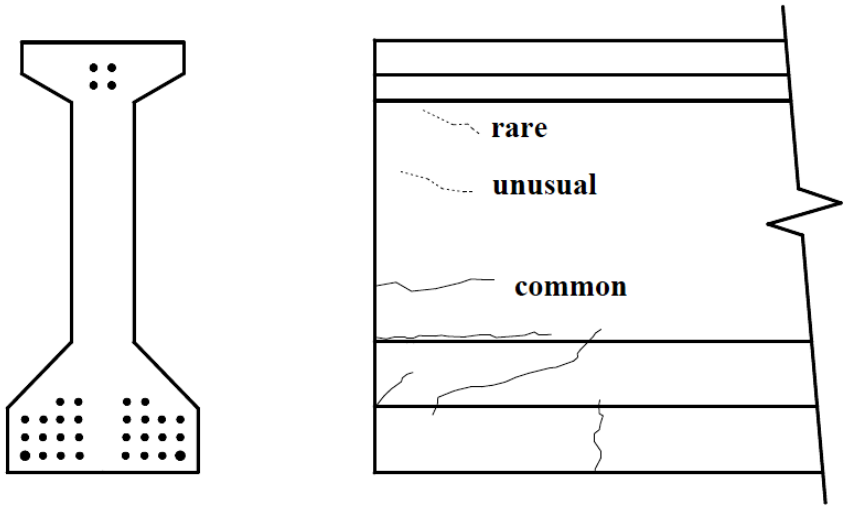

Figure 15. Typically observed end region cracks (adapted from Burgueño and Sun 2011)

APPENDIX A

MATLAB PROGRAM

This Appendix presents the entire MATLAB code used in this study.

The MATLAB program follows the AASHTO-prescribed design procedures and checks. This program was developed for convenient and efficient parametric study. Required input includes girder geometry and strand distribution in addition to some fundamental bridge characteristics including span, girder spacing and slab dimensions. The MATLAB code is used to calculate loads applied to in interior girder (calculating distribution factors) and the appropriate moment and shear envelopes for design. Capacity at critical sections – calculated using AASHTO-prescribed equations - is verified and all appropriate stress limits are calculated. The MATLAB code is not intended for design, but rather to calculate stresses and compare these to appropriate limits. It was developed with the objective of the present work as its goal.

In the file all text following a "%" is an annotation, intended to clarify the code.

```
%Step 1 Input Bridge geometry data
fid_b=fopen('bridge_data.txt');
bridge_data_1=textscan(fid_b,'%s',1);
bridge_data_2=textscan(fid_b,'%f %f %f %f %f %f %f',1);
bridge_data_3=textscan(fid_b,'%f %f %f',1);
girder_type=bridge_data_1{1};          %Girder type (interior or exterior)
L=bridge_data_2{1};                    %Span length (ft.)
S=bridge_data_2{2};                    %Girder spacing (ft.)
ts=bridge_data_2{3};                   %Thickness of deck slab (in.)
ta=bridge_data_2{4};                   %Thickness of wearing surface (in.)
theta=bridge_data_2{5};                %Bridge skew
de=bridge_data_2{6};                   %Exterior overhang (ft.)
support_length=bridge_data_2{7};       %Support length (in.)
weight_girder=bridge_data_3{1};        %Unit weight of girder (lb/ft^3)
weight_slab=bridge_data_3{2};          %Unit weight of deck slab (lb/ft^3)
weight_wearing=bridge_data_3{3};       %Unit weight of wearing surface (lb/ft^3)
fclose(fid_b);

%Girder data
fid_g=fopen('girder_data.txt');
girder_data_1=textscan(fid_g,'%f %f %f %f %f %f',1);
girder_data_2=textscan(fid_g,'%f %f %f %f',1);
girder_data_3=textscan(fid_g,'%f %f %f %f',1);
h=girder_data_1{1};                    %Girder depth (in.)
bv=girder_data_1{2};                   %Girder's web width (in.)
b_flange=girder_data_1{3};             %Girder's flange width (in.)
t_flange=girder_data_1{4};             %Girder's flange thickness (in.)
t_fill=girder_data_1{5};               %Girder's fillet thickness at the top flange (in.)
b_fill=girder_data_1{6};               %Girder's fillet width at the top flange (in.)
w=girder_data_2{1};                    %Self weight (k/ft)
Ag=girder_data_2{2};                   %Cross-section area of non-composite section (in.^2)
Ig=girder_data_2{3};                   %Moment of inertia of non-composite section (in.^4)
Cgb=girder_data_2{4};                  %Distance from the bottom fiber to the centroid (in.)
ydist=girder_data_3{1};                %Distance between layers (in.)
Ap_s=girder_data_3{2};                 %Area of one strand (in.^2)
db=girder_data_3{3};                   %Diameter of strand (in.)
Av=girder_data_3{4};                   %Total stirrup area (in.^2)
fclose(fid_g);

%Material properties
fid_m=fopen('material_data.txt');
material_data=textscan(fid_m,'%f %f %f %f %f %f %f',1);
f_pu=material_data{1};                 %fpu (ksi)
delta_fpr=material_data{2};            %Loss due to relaxation (ksi)
f_yt=material_data{3};                 %yield strength of stirrups (ksi)
fpc_girder=material_data{4};           %f'c for girders (ksi)
fpci=material_data{5};                 %f'c at release (ksi)
fpc_deck=material_data{6};             %f'c for deck slab (ksi)
Ep=material_data{7};                   %Strand modulus of elasticity (ksi)
fclose(fid_m);
%AASHTO factors for analysis & design
fid_AASHTO=fopen('AASHTO_factors.txt');
AASHTO_factors=textscan(fid_AASHTO,'%f %f %f %f %f %f %f',1);
DC=AASHTO_factors{1};                  %DC
DW=AASHTO_factors{2};                  %DW
LL=AASHTO_factors{3};                  %LL
```

```
IM=AASHTO_factors{4};                    %IM
phi_f=AASHTO_factors{5};                 %phi factor for flexure
phi_v=AASHTO_factors{6};                 %phi factor for shear
RH=AASHTO_factors{7};                    %Relative humidity (%)
fclose(fid_AASHTO);

%Stirrups data
%Matrix stirrups gives the length in ft. (the 1st column) over which stirrup
%spacing in inches (the 2nd column) is used
%The last entry is the total stirrup (in.^2)
stirrups=csvread('stirrups.txt');
%Miscellaneous
xincr=0.1;                               %Increments (in ft.) of stations at which values are computed.
tolerance=1e-10;                         %Tolerance for calculations
%Strand data
bonded_debonded = input('Are the strands fully bonded? Y/N [Y]: ', 's');
if isempty(bonded_debonded)
   bonded_debonded = 'Y';
end
if(strcmp(bonded_debonded,'Y')==1)
   xdebond=0;
else
   xdebond=input('Input debond lengths (3 ft. increments are commonly used) :');
end
%Ntotal is the number of bonded strand per layer in each region.
%The size of this matrix is no. of debond regions x no. of rows of strand.
if(strcmp(bonded_debonded,'Y')==1)
   Ntotal=input('Input the no. of bonded strands per layer: ');
else
   Ntotal=input('Input the no. of bonded strands per layer in each region: ');
end


%
%============================Calculations==================================
%Miscellaneous
%calculate the no. of strand layers & no. of debonded regions.
[ndebond,nlayer]=size(Ntotal);

% Step 2 Effective flange width of the composite section (in.)
if(strcmp(girder_type,'interior')==1)
   beff=S*12;
else
   beff=de+0.5*S*12;
end
%beff_temp1=0.25*L*12;
%beff_temp2=12*ts+max(bv,0.5*b_flange);
%beff_temp3=S*12;
%beff=min(min(beff_temp1,beff_temp2),beff_temp3);

% Step 3 kappa for computing development length, ld, for each zone
kappa(1:ndebond)=0;
kappa(1)=1.6;
for i=2:ndebond
   kappa(i)=2.0;
end
```

```
Cgt=h-Cgb;                                  %Distance from the top fiber to the centroid
Sb=Ig/Cgb;                                  %Bottom fiber section modulus
St=Ig/Cgt;                                  %Top fiber section modulus
l_t=60*db/12;                               %Transfer length in ft.
npoints=0.5*L/xincr;                        %No. of points at which calculations are made.
distance=(0:xincr:0.5*L);

% Step 4 Factored self-weights in plf
Girder_weight=(weight_girder*Ag/144)*DC;                %Girder
Slab_weight_I=(ts/12)*S*weight_slab*DC;                 %Slab for interior girders
Slab_weight_E=(ts/12)*(S/2+de)*weight_slab*DC;          %Slab for exterior girders
Wearing_weight_I=(ta/12)*S*weight_wearing*DW;           %Wearing surface for interior girders
Wearing_weight_E=(ta/12)*(S/2+de)*weight_wearing*DW;    %Wearing surface for exterior girders
Weight_I=Girder_weight+Slab_weight_I+Wearing_weight_I;
Weight_E=Girder_weight+Slab_weight_E+Wearing_weight_E;
%
%Convert to klf
Weight_I=Weight_I/1000;
Weight_E=Weight_E/1000;
%
%Calculate the distance from the left support to the end of each region
%with different stirrup spacing.
xtemp=0;
for i=1:length(stirrups)
   xstirrup(i)=stirrups(i,1)+xtemp;
   xtemp=xstirrup(i);
end
%
%============================Analysis ====================================
EG=57000*sqrt(fpc_girder); %Modulus of girder
ED=57000*sqrt(fpc_deck);   %Modulus of deck slab
n=EG/ED;
eg=Cgt+ts/2;
Kg=n*(Ig+Ag*eg^2);
if(Kg<10000||Kg>7000000)
   display('Kg is out of range per AASHTO')
end
%skew correction for shear (AASHTO Table 4.6.2.2.3c-1)
skew_correction_shear=1+0.2*(((12*L*ts^3)/Kg)^0.3)*tand(theta);
%skew correction for moment (AASHTO Table 4.6.2.2.2e-1)
if(theta==0)
   skew_correction_moment=1.0;
else
   c_1=0.25*(Kg/(12*L*ts^3))^0.25*(S/L)^0.5;
   if(theta<30)
      c_1=0.0;
   end
   skew_correction_moment=1-c_1*tand((min(60,theta)))^1.5;
end

%Step 5 Distribution factors
%Interior Girders
DM1_I=0.075+((S/9.5)^0.6)*((S/L)^0.2)*((Kg/(12*L*ts^3))^0.1);       %2+ lanes loaded
DM2_I=0.06+((S/14)^0.4)*((S/L)^0.3)*((Kg/(12*L*ts^3))^0.1);         %1 lane loaded
DMF_I=skew_correction_moment*(DM2_I/1.2);                           %see 3.6.1.1.2
DM_I=skew_correction_moment*max(DM1_I,DM2_I);
```

```
DV1_I=0.2+(S/12)-(S/35)^2;                                  %2+ lanes loaded
DV2_I=0.36+(S/25);                                          %1 lane loaded
DVF_I=skew_correction_shear*(DV2_I/1.2);
DV_I=skew_correction_shear*max(DV1_I,DV2_I);
%Exterior Girders
DM1_E=(0.77+(de/9.1))*DM1_I;                                %2+ lanes loaded
DM2_E=(S-5+de)/S;                                           %1 lane loaded, lever rule (assumed S>6 ft.)
DMF_E=skew_correction_moment*(DM2_E/1.2);
DM_E=skew_correction_moment*max(DM1_E,DM2_E);
DV1_E=(0.6+de/10)*DV1_I;                                    %2+ lanes loaded
DV2_E=DM2_E;                                                %1 lane loaded, lever rule (assumed S> 6 ft.)
DVF_E=skew_correction_shear*(DV2_E/1.2);
DV_E=skew_correction_shear*max(DV1_E,DV2_E);
[DM1_I DM2_I DMF_I DV1_I DV2_I DVF_I];
[DM1_E DM2_E DMF_E DV1_E DV2_E DVF_E];
%Controlling values
[DM_I DMF_I;DM_E DMF_E;DV_I DVF_I;DV_E DVF_E];
%
% Moment
axle1a=(L/2-14-2.33)/L;
axle1b=8;
axle2a=(L/2-2.33)/L;
axle2b=32;
axle3a=(L/2+14-2.33)/L;
axle3b=32;
xpoint=0;
for i=1:npoints+1
   M_Lane(i)=(0.64*xpoint/2)*(L-xpoint)*LL;
   V_Lane(i)=0.64*(0.5*L-xpoint)*LL;
   if(xpoint<(0.5*L-2))
      M_Tandem(i)=25*xpoint;
      V_Tandem_M(i)=25;
   else
      M_Tandem(i)=25*xpoint-25*(xpoint-(L/2-2));
      V_Tandem_M(i)=0;
   end
   if((xpoint/L)<axle1a)
      M1(i)=(1-axle1a)*axle1b*xpoint;
      V1(i)=(1-axle1a)*axle1b;
   else
      M1(i)=(1-axle1a)*axle1b*xpoint-((xpoint/L)-axle1a)*axle1b*L;
      V1(i)=((1-axle1a)*axle1b)-axle1b;
   end
   if((xpoint/L)<axle2a)
      M2(i)=(1-axle2a)*axle2b*xpoint;
      V2(i)=(1-axle2a)*axle2b;
   else
      M2(i)=(1-axle2a)*axle2b*xpoint-((xpoint/L)-axle2a)*axle2b*L;
      V2(i)=((1-axle2a)*axle2b)-axle2b;
   end
   if((xpoint/L)<axle3a)
      M3(i)=(1-axle3a)*axle3b*xpoint;
      V3(i)=(1-axle3a)*axle3b;
   else
      M3(i)=(1-axle3a)*axle3b*xpoint-((xpoint/L)-axle3a)*axle3b*L;
      V3(i)=((1-axle3a)*axle3b)-axle3b;
```

```
    end
    M_H20(i)=M1(i)+M2(i)+M3(i);
    V_H20_M(i)=V1(i)+V2(i)+V3(i);
    M_Lane_Tandem(i)=M_Lane(i)*LL+M_Tandem(i)*LL*IM;
    V_Lane_Tandem_M(i)=V_Lane(i)*LL+V_Tandem_M(i)*LL*IM;
    M_Lane_H20(i)=M_Lane(i)*LL+M_H20(i)*LL*IM;
    V_Lane_H20_M(i)=V_Lane(i)*LL+V_H20_M(i)*LL*IM;
    M_Control(i)=max(M_Lane_Tandem(i),M_Lane_H20(i));
    if(M_Lane_Tandem(i)>M_Lane_H20(i))
       V_Control_M(i)=V_Lane_Tandem_M(i);
    else
       V_Control_M(i)=V_Lane_H20_M(i);
    end
    M_Design_I(i)=M_Control(i)*DM_I;
    VatM_Design_I(i)=V_Control_M(i)*DV_I;
    M_Design_E(i)=M_Control(i)*DM_E;
    VatM_Design_E(i)=V_Control_M(i)*DV_E;
%
% Shear
V1_Tandem(i)=(1-(xpoint/L))*25;
V2_Tandem(i)=(1-((xpoint/L)+(4/L)))*25;
V_Tandem(i)=V1_Tandem(i)+V2_Tandem(i);
V1_H20(i)=(1-(xpoint/L))*32;
V2_H20(i)=(1-((xpoint/L)+(14/L)))*32;
V3_H20(i)=(1-((xpoint/L)+(28/L)))*8;
V_H20(i)=V1_H20(i)+V2_H20(i)+V3_H20(i);
V_Lane_Tandem(i)=V_Lane(i)*LL+V_Tandem(i)*LL*IM;
V_Lane_H20(i)=V_Lane(i)*LL+V_H20(i)*LL*IM;
V_Control(i)=max(V_Lane_Tandem(i),V_Lane_H20(i));
V_Design_I(i)=V_Control(i)*DV_I;
V_Design_E(i)=V_Control(i)*DV_E;
%Dead load moment & shear
M_DL_I(i)=Weight_I*(xpoint/2)*(L-xpoint);
V_DL_I(i)=Weight_I*(0.5*L-xpoint);
M_DL_E(i)=Weight_E*(xpoint/2)*(L-xpoint);
V_DL_E(i)=Weight_E*(0.5*L-xpoint);
%
%Total moments & shears
Total_M_Design_I(i)=M_Design_I(i)+M_DL_I(i);
Total_VatM_Design_I(i)=VatM_Design_I(i)+V_DL_I(i);
Total_M_Design_E(i)=M_Design_E(i)+M_DL_E(i);
Total_VatM_Design_E(i)=VatM_Design_E(i)+V_DL_E(i);
Total_V_Design_I(i)=V_Design_I(i)+V_DL_I(i);
Total_V_Design_E(i)=V_Design_E(i)+V_DL_E(i);
%
%increments along the length
%distance(i)=xpoint;
xpoint=xpoint+xincr;
%
end
%
%Export to Excel for debugging purposes
%xlswrite('check_M.xls',[distance',M_Lane',V_Lane',M_Tandem',V_Tandem_M', ...
%                  M1',M2',M3',M_H20',V1',V2',V3',V_H20',M_Lane_Tandem', ...
%                  V_Lane_Tandem_M',M_Lane_H20',V_Lane_H20_M',...
%                  M_Control',V_Control_M',M_Design_I',VatM_Design_I', ...
```

```
%                   M_Design_E',VatM_Design_E'])
%xlswrite('check_V.xls',[distance',V1_Tandem',V2_Tandem',V_Tandem', ...
%                   V1_H20',V2_H20',V3_H20',V_H20',V_Lane_Tandem',V_Lane_H20',...
%                   V_Control',V_Design_I',V_Design_E'])
%xlswrite('check_V&M.xls',[distance',M_DL_I',V_DL_I',M_DL_E',V_DL_E',...
%                    Total_M_Design_I',Total_VatM_Design_I', ...
%                    Total_M_Design_E',Total_VatM_Design_E',...
%                    Total_V_Design_I',Total_V_Design_E'])
%
%======================Analysis related to debonding======================
%Compute the percentage of debonded strands
%Compute the no. of bonded strands in each region
for i=1:ndebond
   ndebond_region(i)=sum(Ntotal(i,1:end));
end
%
%Compute the precentage of debonded strands in each region
for i=1:ndebond
   percentdebond_perregion(i)=(ndebond_region(ndebond)-ndebond_region(i))/ ...
      ndebond_region(ndebond);
end
%Compute the percentage of debonded strands in each row for each region
for i=1:ndebond
   for j=1:nlayer
      percentdebond_perrow(i,j)=(Ntotal(ndebond,j)-Ntotal(i,j))/Ntotal(ndebond,j);
   end
end
if(strcmp(bonded_debonded,'Y')==1)
   xlswrite('percentdebond_perregion_bonded.xls',[percentdebond_perregion])
   xlswrite('percentdebond_perrow_bonded.xls',[percentdebond_perrow])
else
   xlswrite('percentdebond_perregion_debonded.xls',[percentdebond_perregion])
   xlswrite('percentdebond_perrow_debonded.xls',[percentdebond_perrow])
end
%percentdebond_perregion
%percentdebond_perrow
%
%Compute the distance from the left support to each region.
temp=0;
xL(1)=0;
for i=2:ndebond
   xL(i)=xdebond+temp;
   temp=xL(i);
end
%
%Compute the distance to centroid of each layer
temp=0;
for i=1:nlayer
   y(i)=temp+ydist;
   temp=y(i);
end
%
%Calculate the centroid of strands in each region (measured from the bottom fiber)
for i=1:ndebond
   Nsum(i)=0;
   As_times_y=0;
```

```
   Aps(i)=0;
   for j=1:nlayer
      Nsum(i)=Nsum(i)+Ntotal(i,j);
      As_times_y=As_times_y+y(j)*Ntotal(i,j);
   end
   Aps(i)=Nsum(i)*Ap_s;    %Total area of prestressing steel in each region
   ybs(i)=As_times_y/Nsum(i);
   e(i)=Cgb-ybs(i);
end
%
%Compute the incremental area of prestressing steel in each region
Apsincr(1)=Aps(1);
for i=2:ndebond
   Apsincr(i)=Aps(i)-Aps(i-1);
end
%
%Step 6 Compute various losses
f_py=0.9*f_pu;
f_pbt=0.75*f_pu;
f_pi=0.75*f_pu;
gama_h=1.7-0.01*RH;                                    %AASHTO Eq. 5.9.5.3-2
gama_st=5/(1+fpci);                                    %AASHTO Eq. 5.9.5.3-3
Aps_total=Aps(ndebond);
delta_fpLT=(10.0*f_pi*Aps_total*gama_h*gama_st/Ag)+(12*gama_h*gama_st) ...
        +delta_fpr;
em=Cgb-ybs(ndebond);                                   %average prestressing steel eccentricity @ midspan
Eci=1820*sqrt(fpci);
Mg_midspan=12*(L^2*w)/8;    %midspan moment due to self-weight
delta_fpES=(Aps_total*f_pbt*(Ig+em^2*Ag)-em*Mg_midspan*Ag)/ ...
        (Aps_total*(Ig+em^2*Ag)+(Ag*Ig*Eci/Ep));       %AASHTO Eq. (C5.9.5.2.3a-1)
delta_fpT=delta_fpLT+delta_fpES;
f_pe=f_pbt-delta_fpT;
f_pt=0.75*f_pu*(1-0.07);
%

%Step 7 Compute f_ps & Mn
k=2*(1.04-(f_py/f_pu));                                %AASHTO Eq. 5.7.3.1.1-2
if(fpc_deck<=4)
   beta1_deck=0.85;
else
   beta1_deck=max(0.65,(0.65-0.2*(fpc_deck-8)));
end
if(fpc_girder<=4)
   beta1_girder=0.85;
else
   beta1_girder=max(0.65,(0.65-0.2*(fpc_girder-8)));
end
beta1avg=0.5*(beta1_deck+beta1_girder);
for i=1:ndebond
   dp=h+ts-ybs(i);
%
   c1=(Aps(i)*f_pu)/((0.85*fpc_deck*beff*beta1avg)+ ...
     (k*Aps(i)*f_pu/dp));
%
   Cforce1_2=0.85*fpc_deck*ts*beff;
   num2=Aps(i)*f_pu-Cforce1_2+0.85*fpc_girder*b_flange*ts;
```

```
   denom2=0.85*fpc_girder*beta1avg*b_flange+k*Aps(i)*f_pu/dp;
   c2=num2/denom2;
%
   Cforce1_3=0.85*fpc_deck*beff*ts;
   Cforce2_3=0.85*fpc_girder*b_flange*t_flange;
   num3=0.85*fpc_girder*(ts+t_flange)*bv+Aps(i)*f_pu-Cforce1_3-Cforce2_3;
   denom3=0.85*fpc_girder*beta1avg*bv+(Aps(i)*f_pu*k/dp);
   c3=num3/denom3;
%
   Cforce1_4=0.85*fpc_deck*beff*ts;
   Cforce2_4=0.85*fpc_girder*b_flange*t_flange;
   Cforce3_4=0.85*fpc_girder*t_fill*(bv+b_fill);
   num4=Aps(i)*f_pu+0.85*fpc_girder*(ts+t_flange+t_fill)*bv- ...
       Cforce1_4-Cforce2_4-Cforce3_4;
   denom4=(0.85*fpc_girder*beta1avg*bv)+(f_pu*k*Aps(i)/dp);
   c4=num4/denom4;
%If c is within the thickness of the deck slab
   if(c1<=ts)
      NA(i)=c1;
      f_ps(i)=f_pu*(1-k*c1/dp);
      a1=beta1_girder*c1;
      Mn(i)=Aps(i)*f_ps(i)*(dp-0.5*a1);
   end
%If c is flange beam flange thickness.
   if(c2>ts&&(c2-(ts+t_flange))<tolerance)
      NA(i)=c2;
      f_ps(i)=f_pu*(1-k*c2/dp);
      a2=beta1avg*c2;
      T=Aps(i)*f_ps(i);
      Cforce=0.85*fpc_girder*b_flange*(beta1avg*c2-ts);
      Mn(i)=T*(dp-0.5*ts)-Cforce*0.5*a2;
   end
%If c is within the tapered portion.
    if(c3>(ts+t_flange)&&(c3-(ts+t_flange+t_fill))<tolerance)
       NA(i)=c3;
       f_ps(i)=f_pu*(1-k*c3/dp);
       a3=beta1avg*c3;
       Cforce3_3=0.85*fpc_girder*(beta1avg*c3-ts-t_flange)*bv;
       T=Cforce1_3+Cforce2_3+Cforce3_3;
       Mn(i)=T*(dp-0.5*ts)-Cforce2_3*(0.5*ts+0.5*t_flange)- ...
            Cforce3_3*(0.5*a3+0.5*t_flange);
    end
%If c is within the web.
    if(c4>(ts+t_flange+t_fill))
       NA(i)=c4;
       f_ps(i)=f_pu*(1-k*c4/dp);
       a4=beta1avg*c4;
       Cforce4_4=0.85*fpc_girder*(beta1avg*c4-ts-t_flange-t_fill)*bv;
       T=Cforce1_4+Cforce2_4+Cforce3_4+Cforce4_4;
       Mn(i)=T*(dp-0.5*ts)-Cforce2_4*(0.5*ts+0.5*t_flange)- ...
           Cforce3_4*(((t_fill*(2*b_flange+bv))/(3*(b_flange+bv)))+t_flange+0.5*ts)- ...
           Cforce4_4*(0.5*a4+0.5*ts+0.5*t_fill);
     end
end
%
%Step 8 Compute various stresses along the span
```

```
for i=1:npoints+1
   x=distance(i);
   P_pt(i)=0;
   fpoAps(i)=0;
   fpsAps(i)=0;
   Aps_overlength(i)=0;
   Mg(i)=0.5*w*x*(L-x);
   for j=1:ndebond
      if(x>=xL(j))
         dist=x-xL(j);
         fpt(i,j)=min(f_pt,dist*f_pt/l_t);
         fpo(i,j)=min(dist*0.7*f_pu/l_t,0.7*f_pu);
         P_pt(i)=P_pt(i)+Apsincr(j)*fpt(i,j);
         fpoAps(i)=fpoAps(i)+Apsincr(j)*fpo(i,j);
         f_top(i)=(Mg(i)*12/St)+(P_pt(i)/Ag)-(P_pt(i)*e(j)/St);
         f_bottom(i)=-(Mg(i)*12/Sb)+(P_pt(i)/Ag)+(P_pt(i)*e(j)/Sb);
         if(dist<=l_t)
            fps(i,j)=min((dist*f_pe/l_t),f_pe);
         else
            l_d=(1/12)*kappa(j)*(f_ps(j)-(2/3)*f_pe)*db;
            fps(i,j)=min(f_ps(j),(f_pe+(dist-l_t)*(f_ps(j)-f_pe)/(l_d-l_t)));
         end
         fpsAps(i)=fpsAps(i)+Apsincr(j)*fps(i,j);
         Aps_overlength(i)=Aps_overlength(i)+Apsincr(j);
      end
   end
end
%
%Export to Excel for debugging purposes
%xlswrite('check_stresses.xls',[distance',P_pt',f_top',f_bottom',fpoAps',...
%                        Aps_overlength',fpsAps'])
%

%Step 9 Check the effects of debonding on shear capacity
Mu(1:length(distance))=0;
Vu(1:length(distance))=0;
MuDesign(1:length(distance))=0;
if(strcmp(girder_type,'interior')==1)
   Mu=M_Design_I;
   MuDesign=Total_M_Design_I;
   Vu=VatM_Design_I;
%    Mu=Total_M_Design_I;
%    Vu=Total_VatM_Design_I;
else
   Mu=M_Design_E;
   MuDesign=Total_M_Design_E;
   Vu=VatM_Design_E;
%    Mu=Total_M_Design_E;
%    Vu=Total_VatM_Design_E;
end
dv=0.72*h;                                          %Assume dv=0.72h
%Calculate strirrup spacing along the length
istart=1;
for i=1:length(distance)
   vu=Vu(i)/(bv*dv);
   if(vu<0.125*fpc_girder)
```

```
      s_max(i)=min(24,0.8*dv);
   else
      s_max(i)=min(12,0.4*dv);
   end
   if(distance(i)<=xstirrup(end))
      if((distance(i)-xstirrup(istart))<=tolerance)
         Stirrup_s(i)=min(s_max(i),stirrups(istart,2));
      else
         istart=istart+1;
         Stirrup_s(i)=min(s_max(i),stirrups(istart,2));
      end
   else
%       spacing=min(s_max,stirrups(istart,2))
      Stirrup_s(i)=s_max(i);
   end

end
for i=1:length(distance)
   temp=(abs(Mu(i)*12/dv)+abs(Vu(i))-fpoAps(i))/(Aps_overlength(i)*Ep);
   epsilon(i)=max(0,temp);
   beta(i)=4.8/(1+750*epsilon(i));
   theta(i)=29+3500*epsilon(i);
   v_c(i)=0.0316*beta(i)*sqrt(fpc_girder);
   V_c(i)=v_c(i)*bv*dv;
   V_s(i)=(Av*f_yt*dv/Stirrup_s(i))*(1/tand(theta(i)));
   V_n(i)=min((V_c(i)+V_s(i)),(0.25*fpc_girder*bv*dv));
   T_force(i)=(Mu(i)*12)/(dv*phi_f)+(1/tand(theta(i)))*((Vu(i)/phi_v)-0.5*V_s(i));
   fpsAps_over_T_force(i)=fpsAps(i)/T_force(i);
end
%
%Check the flexural capacity
ratio=phi_f*Mn(ndebond)/(max(MuDesign)*12);
str = ['phiMn/Mu = ',num2str(ratio)]
%
%Export to Excel for debugging purposes
%xlswrite('checks_Vc,Vs,T.xls',[distance',Mu',Vu',epsilon',beta',theta',v_c',...
%                              V_c',V_s',T_force',fpsAps_over_T_force'])
%
%Perform the following tasks only if the girder has adequate flexural
%capacity.
if(ratio>(1+tolerance))
%Strut angle at critical section near the support.
angle=interp1(distance,theta,(0.5*support_length/12),'cubic');
%
%Location of critical section near the support.
distance_at_support=(0.5*support_length/12)+ybs(1)*(1/tand(angle))/12;
%
%Export data for further ploting in Excel
if(strcmp(bonded_debonded,'Y')==1)
   xlswrite('fpsAps_T_bonded.xls',[[0;0;distance'],[dv;distance_at_support;fpsAps_over_T_force']
      ])
else
   xlswrite('fpsAps_T_debonded.xls',[[0;0;distance'],[dv;distance_at_support;fpsAps_over_T_force']
      ])
end
%
```

APPENDIX B

REPRESENTATIVE PROTOTYPE EXAMPLE - CASE B29

This example presents the capacity calculation for the partially debonded girder of Case B29 described in Section 3.3 and Table 3-7. Capacity calculations were made using the MATLAB program described in Appendix A, which follows the methodology of AASHTO *LRFD Specification* (2010).

STEP 1: INPUT SECTIONAL AND MATERIAL PROPERTIES

Girder properties

Span Length:	105 ft.
Spacing :	6 ft
Skew :	0 degrees
Prestressing Steel:	0.6 in. diameter, 270 ksi low-lax strands
Total No. of strands in mid-span:	26
Concrete Compressive Strength:	f_c' = 8 ksi for the girder and 4 ksi for the slab

Section properties

AASHTO Type IV Girder:	A_{cg} = 789 in^2
	I_x = 260,730 in^4
	y_b = 24.73 in.
	Unit weight = 150 psf
Slab:	t_s = 8 in.
	S = 6 ft.
	Unit weight = 150 psf
Wearing surface:	t = 3 in.
	Unit weight = 125 psf

STEP 2: EFFECTIVE WIDTH

The effective flange width: LRFD 4.6.2.6.1

$$b_i = \min\left\{\begin{array}{c} \frac{L}{4} \\ 12\mathrm{t}_s + \max(b_w, \frac{1}{2}b_f) \\ center - to - center\_girder\_spacing \end{array}\right\}$$

$$= \min\left\{\begin{array}{l} \frac{105}{4}\ ft. \\ 12\times 8in. + \frac{1}{2}\times 26in. \\ 6\ ft. \end{array}\right\} = 72\text{in.}$$

STEP 3: DEAD LOAD ANALYSIS

Components and Attachment: DC

Girder self-weight: = (150×789/144)×1.25 = 1027 lb/ft

Slab self-weight: (8/12)×6×150×1.25 = 750 lb/ft

Wearing Surface: DW

Asphalt thickness = 3 in.: (3/12)×6×125×1.5 = 281 lb/ft

Total Weight: DC+DW

Total weight: 1027+750+281 = 2059 lb/ft = 2.059 klf.

STEP 4: COMPUTE LIVE LOAD DISTRIBUTION FACTORS FOR INTERIOR GIRDERS

Longitudinal Stiffness Parameter:

$K_g = n(I+Ae_g^2) = 1.604\times10^6$ LRFD 4.6.2.2.1

Distribution Factor for Moment – Interior Girders, $mg_{M,IN}$:

One Lane Loaded: LRFD T4.6.2.2.2b-1

$$mg_M^{SI} = 0.06 + \left(\frac{S}{14}\right)^{0.4}\left(\frac{S}{L}\right)^{0.3}\left(\frac{K_g}{12.0Lt_s^3}\right)^{0.1} = 0.544$$

Two Lanes Loaded:

$$mg_M^{MI} = 0.075 + \left(\frac{S}{9.5}\right)^{0.6}\left(\frac{S}{L}\right)^{0.2}\left(\frac{K_g}{12.0Lt_s^3}\right)^{0.1} = 0.391$$

$mg_{M,IN} = 0.544$

Distribution Factor for Shear – Interior Girders, $mg_{V,IN}$:

One Lane Loaded: LRFD T4.6.2.2.3a-1

$$mg_V^{SI} = 0.36 + \frac{S}{25.0} = 0.600$$

Two Lanes Loaded:

$$mg_V^{MI} = 0.2 + \frac{S}{12} - \left(\frac{S}{35}\right)^{2.0} = 0.671$$

$mg_{V,IN} = 0.671$

STEP 5: LIVE LOAD ANALYSIS

	Moment (HL-93)	***Shear (HL-93)***
LANE LOAD	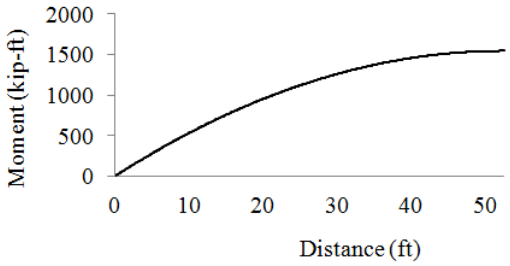	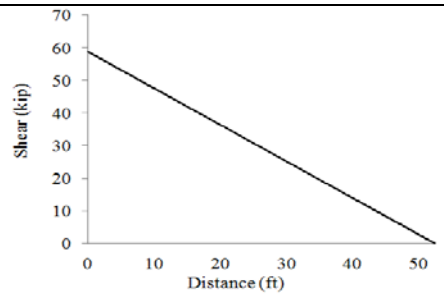
TANDEM	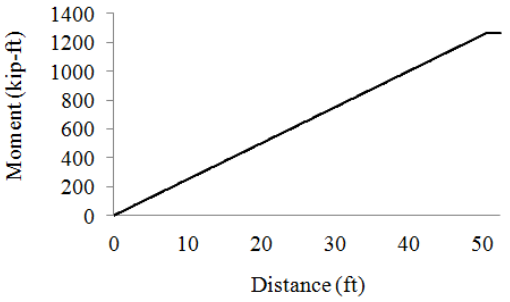	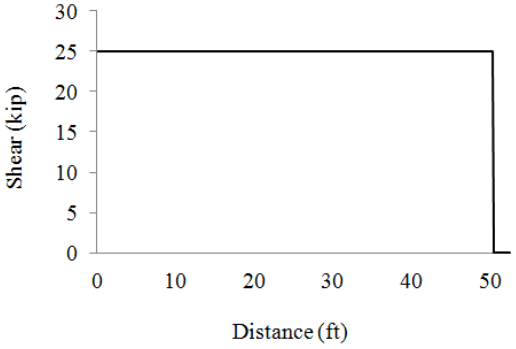
TRUCK	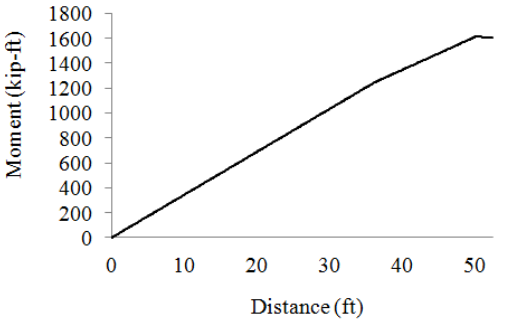	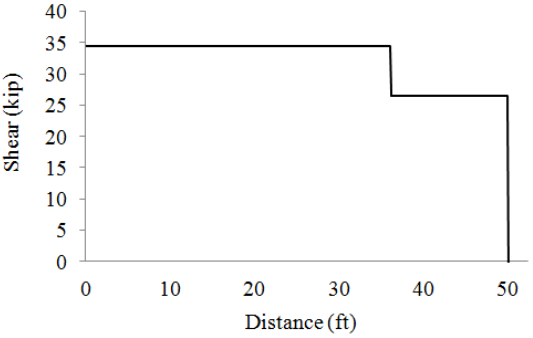
DESIGN	IM = 33% (LRFD T3.6.2.1-1) $M_{Design} = mg_{M,IN} \times M_{LL+IM}$ $= 0.544M_{LL+IM}$	IM = 33% (LRFD T3.6.2.1-1) $V_{Design} = mg_{V,IN} \times V_{LL+IM}$ $= 0.671V_{LL+IM}$

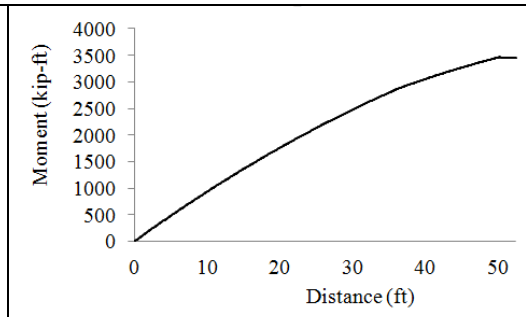

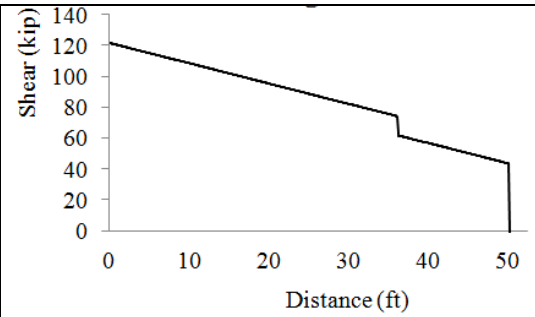

STEP 6: EFFECTIVE PRESTRESS

Determine Effective Prestress, P_{pe}:

$P_{pe} = A_{ps} \times f_{pe}$

Total Prestress Losses: LRFD Eq. 5.9.5.1-1

$\Delta f_{pT} = \Delta f_{pT} + \Delta f_{pLT}$ immediately before transfer

Effective Prestress Losses:

f_{pe} = Initial Prestress - Total Prestress Losses

Loss due to elastic shorting, Δf_{pES}:

$$\Delta f_{pES} = \frac{A_{ps} f_{pbt}(I_g + e_m^2 A_g) - e_m M_g A_g}{A_{ps}(I_g + e_m^2 A_g) + \frac{A_g I_g E_{ci}}{E_p}}$$ = 12.2 ksi LRFD Eq. C5.9.5.2.3a-1

Approximate lump sum estimate of time-dependent losses

$$\Delta f_{pLT} = 10.0 \frac{f_{pi} A_{ps}}{A_g} \gamma_h \gamma_{st} + 12.0 \gamma_h \gamma_{st} + \Delta f_{pR}$$ = 19.2 ksi LRFD Eq. 5.9.5.3-1

with H = 70%; $\gamma_h = 1.7 - 0.01H = 1.7 - 0.01 \times 70 = 1.0$ LRFD Eq. 5.9.5.3-2

$$\gamma_{st} = \frac{5}{(1 + f_{ci}^{'})} = \frac{5}{(1 + 6.8)} = 0.641$$ LRFD Eq. 5.9.5.3-3

Δf_{pR} = an estimate of relaxation loss = 2.4 ksi

f_{pi} = 0.75 x 270 = 202.5 ksi

Total Prestress Losses, Δf_{pT}:

$$\Delta f_{pT} = \Delta f_{pLT} + \Delta f_{pES} = 31.5 ksi$$

Effective Strength in strands, f_{pe}:

$$f_{pe} = 0.75 f_{pu} - \Delta f_{pT} = 0.75 \times 270 - 31.5 = 171 ksi$$

STEP 7: COMPUTE NOMINAL FLEXURAL RESISTANCE

Average stress in prestressing steel at nominal resistance of member:

$$f_{ps} = f_{pu}(1 - k\frac{c}{d_p})$$ LRFD Eq.5.7.3.1.1-1

f_{pu} = 270 ksi and k = 0.28 for low lax strands

d_p = distance from extreme compression fiber to C.G. of prestressing tendons:

d_p = 54+8 – 3.8 = 58.2 in.

At mid-span, A_{ps} = 26 × 0.215 = 5.59 in.^{2}

$$c = \frac{A_{ps} f_{ps} - A_s f_s - A_s' f_s'}{0.85 f_c' \beta_1 b + k A_{ps} \frac{f_{pu}}{d_p}} = \frac{5.59 \times 270 - 0}{0.85 \times 4 \times 72 \times 0.75 + \frac{0.28 \times 5.59 \times 270}{58.2}}$$ LRFD Eq. 5.7.3.1.1-4

= 7.9in.

a = β_1c = 0.75 × 7.9 = 5.93 in. < 8 in.

Therefore, rectangular section behavior assumption is valid

$$f_{ps} = 270 \times (1 - 0.28 \times \frac{7.9}{58.2}) = 259.7 \text{ ksi}$$

$$M_n = A_{ps} f_{ps}(d_p - \frac{a}{2}) = 5.59 \times 259.7 \times (58.2 - \frac{5.93}{2})$$ LRFD Eq. 5.7.3.2.2-1

$$= 8.07 \times 10^4 kip - in. = 6725 kip - ft$$

STEP 8: CHECK THE STRESS DUE TO SELF -WEIGHT

Moment due to girder self-weight: 0.822×1052/8 = 1132.8 kip-ft

At mid-span, F_i = 1052.7 kip, e_m = 24.73- 3.86 = 20.9 in.

The tensile stress at the top of the girder is:

$$f_{ti} = -\frac{F_i}{A_g} + \frac{F_i e_m}{S_{tg}} - \frac{M_{dg}}{S_{tg}} = -\frac{1052.7}{789} + \frac{1052.7 \times 20.9}{8907.8} - \frac{1132.8 \times 12}{8907.8} = 0.39\text{ksi} < 0.65\text{ksi}...\text{Satisfied}$$

The compressive stress at the bottom of the girder is:

$$f_{bi} = -\frac{F_i}{A_g} - \frac{F_i e_m}{S_{bg}} + \frac{M_{dg}}{S_{bg}} = -\frac{1052.7}{789} - \frac{1052.7 \times 20.9}{10543} + \frac{1132.8 \times 12}{10543} = 2.13 ksi < 4.08 ksi...\text{Satisfied}$$

The top and bottom stresses along the whole girder are shown in Figure 3-6.

STEP 9: CHECK THE DEBONDING ON SHEAR

The spacing of stirrup is 24in. along the whole girder.

$$V_c = 0.0316\beta\sqrt{f_c'} b_v d_v = 0.0316 \times 4.4436 \times \sqrt{8} \times 8 \times 38.88 = 123.5\text{kip}$$ LRFD Eq.5.8.3.3-3

$$V_s = \frac{A_v f_y d_v \cot\theta}{s} = 69.1 kip$$ LRFD Eq.5.8.3.3-4

$$V_n = \min\begin{Bmatrix} V_s + V_c \\ 0.25 f_c' b_v d_v \end{Bmatrix} = 192.6 kip$$ LRFD Eq.5.8.3.3.-1/-2

$$\frac{A_{ps} f_{ps}}{\frac{|M_u|}{d_v \phi_f} + \cot\theta(\left|\frac{V_u}{\phi_v}\right| - 0.5V_s)} = \frac{1469.5 kip}{986.7 kip} = 1.49 \geq 1...Satisified$$ LRFD Eq.5.8.3.5-1

Shear resistance along the whole girder is shown in Figure 3-7a. At the sections near the support, shear failure may be expected.

REFERENCES

American Association of State Highway and Transportation Officials (AASHTO). 2010. *LRFD Bridge Design Specifications*, 5th Edition and Interims, Washington, D.C.

Abdalla, O.A., Ramirez J.A., and Lee R.H. (1993). "Strand Debonding in Pretensioned Beams - Precast Prestressed Concrete Bridge Girders with Debonded Strands - Continuity Issues," *Joint Highway Research Project FHWA/IN/JHRP-92/24*, doi: 10.5703/1288284314206.

Barnes, R., Burns, N., and Kreger, M.(1999). "Development Length of 0.6-Inch Prestressing Strand in Standard I-Shaped Pretensioned Concrete Beams," *FHWA/TX-02/1388-1, Research Report 1388-1*.

Baxi, A. (2005). "Analytical modeling of fully bonded and debonded pre-tensioned prestressed concrete members," *Doctoral Thesis*, University of Texas at Austin.

Burgueño, R., Sun, Y., (2011). "Effects of Debonded Strands on the Production and Performance of Prestressed Concrete Beams," *Research Report* for MDOT under Contract, No. 2006-0411/7 SPR No. 87346, Michigan State University**.**

Ghosh, S.K., and Finte, M. (1986). "Development Length of Prestressing Strands, Including Debonded Strands, and Allowable Concrete Stresses in Pretensioned Members," *PCI Journal/Sep.-Oct.*, Special Funded R&D Program, PCISFRAD Project No. 2, p.38-27.

Hoyer E. (1939). "Der Stahlsaitenbeton [piano-string-concrete]". *Otto Elsner, Berlin*; 1939. p. 136 [in German].

Kaar, P. H., and Magura, D. (1965). "Effect of strand blanketing on performance of pretensioned girders." *PCI Journal*, 10(6), 20-34.

Kasan J. L. (2012). "On the Repair of Impact-Damaged Prestressed Concrete Bridge Girders," *Doctoral Thesis*, University of Pittsburgh.

Leonhardt, F. (1964). *Prestressed Concrete: Design and Construction*, Wilhem Ernst & Sohn, Berlin.

Ma, Z., Tadros, M.K., and Baishya, M. (1999). "Shear Strength of High Performance Concrete (HPC) I-Girders," *First Engineering Foundation Conference on High Strength Concrete*, p. 257-269.

Oliva, M.G. and Okumus, P. (2011). "Finite Element Analysis of Deep Wide-Flanged Pre-stressed Girders to Understand and Control End Cracking," *WHRP 11-06, Final Report*.

PCI Bridge Design Manual. 2011. 3rd Edition. The PCI Bridge Design Manual Steering Committee, part of the Transportation Activities Council, Precast/Prestressed Concrete Institute, ISBN: 978-0-9846705-4-3.

Rabbat, B.G., Kaar P. H., Russell, H. G. and Bruce, R. N. (1979). "Fatigue Tests of Pretensioned Girders with Blanketed and Draped Strands," *PCI Journal*, PCA R&D Ser. 1621, p.88-114.

Russell, B.W. and Burns, N.H. (1993). "Design Guidelines for Transfer, Development and Debonding of Large Diameter Seven Wire Strands in Pretensioned Concrete Girders. Final Report," *FHWA/TX-93+1210-5F*.